AD NUMBER
AD335203
CLASSIFICATION CHANGES
TO: **UNCLASSIFIED**
FROM: **CONFIDENTIAL**
LIMITATION CHANGES
TO: **Approved for public release; distribution is unlimited.**
FROM: **Distribution authorized to U.S. Gov't. agencies and their contractors; Administrative/Operational Use; JAN 1963. Other requests shall be referred to Air Force Arnold Engineering Development Center, Arnold AFB, TN.**
AUTHORITY
22 DEC 1975 aedc, per document marking; aedc per document marking

AD NUMBER
AD335203
CLASSIFICATION CHANGES
TO: **CONFIDENTIAL**
FROM: **SECRET**
AUTHORITY
6 feb 1975 aedc, per document marking

DECLASSIFIED / UNCLASSIFIED UNCLASSIFIED

AEDC-TDR-62-224 [redacted]

UNCLASSIFIED [redacted]

CLASSIFICATION CANCELLED
BY AUTHORITY OF AF letter dtd 29 Dec 75

Name and Position of Individual

Date 4/14/76

ARO, INC.
DOCUMENT CONTROL
NO IG-298-343
COPY 1 OF 140
SERIES A PAGES 46

119478

(TITLE UNCLASSIFIED)

JAN 3 1964

WIND TUNNEL STUDIES OF ROCKET ENGINE PLUME INFRARED RADIATION IN SUPERSONIC FLOW

JUN 26 1964

...ent has been approved for ... distribution is unlimited.

DEC 28 1964

6-15-65

By

P. D. Gerke and L. L. Galigher
Propulsion Wind Tunnel Facility
ARO, Inc.

DEC 8 1965

1 JUL 1966

NATIONAL SECURITY INFORMATION
Unauthorized Disclosure Subject to Criminal Sanctions

JAN 17 1967

TECHNICAL DOCUMENTARY REPORT NO. AEDC-TDR-62-224

MAY 19..

January 1963

JAN 1968

JUN 1969

JUN 1970

JUN 1971

JUL 1972

AFSC Program Area 920F

[illegible]

(Prepared under Contract No. AF 40(600)-1000 by ARO, Inc., contract operator of AEDC, Arnold Air Force Station, Tenn.)

JUN 1973

JUN 1974

ARNOLD ENGINEERING DEVELOPMENT CENTER

AIR FORCE SYSTEMS COMMAND

UNITED STATES AIR FORCE

[redacted]

... has been approved for public release; its distribution is unlimited.

DECLASSIFIED / UNCLASSIFIED

UNCLASSIFIED [redacted]

EXCLUDED FROM THE ...

Date CLASSIFICATION CHANGED TO Confidential
BY AUTHORITY OF
BY Name and Position of Individual
Date

NOTICES

Qualified requesters may obtain copies of this report from ASTIA. Orders will be expedited if placed through the librarian or other staff member designated to request and receive documents from ASTIA.

When Government drawings, specifications or other data are used for any purpose other than in connection with a definitely related Government procurement operation, the United States Government thereby incurs no responsibility nor any obligation whatsoever; and the fact that the Government may have formulated, furnished, or in any way supplied the said drawings, specifications, or other data, is not to be regarded by implication or otherwise as in any manner licensing the holder or any other person or corporation, or conveying any rights or permission to manufacture, use, or sell any patented invention that may in any way be related thereto.

This document contains information affecting the national defense of the United States within the meaning of the Espionage Laws (Title 18, U.S.C., sections 793 and 794) the transmission or revelation of which in any manner to an unauthorized person is prohibited by law.

(Title Unclassified)
WIND TUNNEL STUDIES OF ROCKET ENGINE PLUME INFRARED RADIATION IN SUPERSONIC FLOW

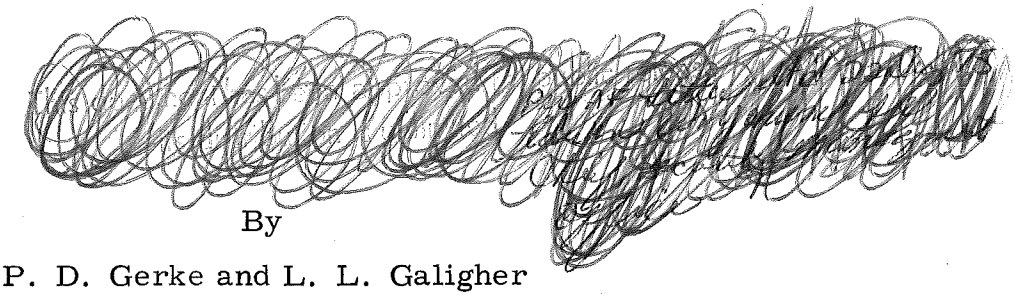

By

P. D. Gerke and L. L. Galigher

Propulsion Wind Tunnel Facility

ARO, Inc.

a subsidiary of Sverdrup and Parcel, Inc.

January 1963

ARO Project No. PS0133

FOREWORD

The authors wish to acknowledge the assistance of Mr. J. W. Cunningham and Mr. G. J. Gardner in reducing the data presented in this report.

(This abstract is classified [redacted])

ABSTRACT

Infrared radiation measurements of rocket engine plumes, taken at a wavelength of 2.645 microns, were obtained in the 16-Ft Supersonic Tunnel of the Propulsion Wind Tunnel Facility at the Arnold Engineering Development Center. Two rocket nozzle-exit area ratios (8 to 1 and 25 to 1) and two propellant combinations (oxygen/RP-1 and oxygen/hydrogen) were used in the investigation.

Results concerning the effect of trajectory conditions and equivalence ratio upon the plume radiation emission are presented in this report. Relative radiation levels for the quenched and unquenched rocket plumes are presented for several test trajectory conditions.

Infrared radiation levels were significantly higher at Mach number and altitude conditions than at static sea-level conditions for the same equivalence ratio. Increasing fuel richness increased the radiance levels at static sea-level conditions. The radiance produced by the oxygen/RP-1 and oxygen/hydrogen propellants were essentially the same for approximately the same equivalence ratio.

Quenching by peripheral injection of RP-1 fluid normal to the rocket exhaust was effective in reducing both the visible rocket plume and the infrared radiation.

(Catalog cards with an unclassified abstract may be found in the back of this document.)

PUBLICATION REVIEW

This report has been reviewed and publication is approved.

A. Lincoln Coapman
Major, USAF
Acting AF Representative, PWT
DCS/Test

Jean A. Jack
Colonel, USAF
DCS/Test

CONTENTS

TABLES

ILLUSTRATIONS

NOMENCLATURE

M_∞	Free-stream Mach number
N_λ	Spectral radiance, watt cm^{-2} $ster^{-1}$ $micron^{-1}$
O/F	Oxidizer-fuel ratio by weight
(O/F)*	Stoichiometric O/F ratio by weight: Oxygen/RP-1: (O/F)* = 3.38 Oxygen/Hydrogen: (O/F)* = 8.00
r_e	Rocket nozzle exit radius, in.
T_{t_∞}	Free-stream stagnation temperature, °R
wp	Total rocket propellant weight flow, lb/sec
wq	Quench liquid weight flow, lb/sec
x	Axial distance from the rocket engine exit, positive downstream, in.
y	Radial distance from the rocket engine centerline, (positive left looking downstream), in.
Z	Altitude, ft
μ	Wavelength, micron
Φ	Equivalence ratio (ratio of stoichiometric O/F ratio to test O/F ratio)

1.0 INTRODUCTION

At the request of the Space Systems Division (SSD), Air Force Systems Command (AFSC), under authorization from the Advanced Research Projects Agency (ARPA), characteristics of the exhausts of small rocket engines were determined for the Convair Division of General Dynamics Corporation. Pressure, temperature, gas composition, and radiation measurements of rocket engine plumes were made during tests conducted between December 7, 1961, and January 5, 1962, in the 16-Ft Supersonic Tunnel of the Propulsion Wind Tunnel Facility (PWT) at the Arnold Engineering Development Center (AEDC), AFSC.

The research program had several objectives. One of these was to study the pressure, temperature, and gas composition distributions of a rocket jet, particularly the interaction region between a fuel rich jet and a surrounding supersonic stream. Other objectives were to study the radiation emission of the plume (plume mapping phase) and to determine the degree of reduction of infrared radiation and visible flame extinguishment resulting from injecting RP-1 into the rocket exhaust (plume quenching phase).

Some results of rocket plume temperature, pressure, and gas composition distribution are presented in Ref. 1. Presented in this report are results regarding the infrared radiation investigations.

2.0 APPARATUS

2.1 TEST FACILITY

The PWT 16-Ft Supersonic Tunnel is a continuous flow, closed circuit wind tunnel. The tunnel is designed to operate at stagnation pressures of approximately 100 to 2,000 psfa. A flexible nozzle provides an operating Mach number range of 1.5 to 4.0 with a maximum operating stagnation air temperature of 650°F. The tunnel employs a scavenging system to remove exhaust gases and a makeup air system to supply conditioned air through an atmospheric drier to maintain equilibrium tunnel conditions. The PWT 16-Ft Supersonic Tunnel and the associated support equipment are shown in Fig. 1. A complete description of the tunnel is given in Ref. 2. Shown in Fig. 2 is the location of the basic test installation in the tunnel.

Manuscript released for printing January 1963.

2.2 ROCKET ENGINES

The rocket engines used in the test are shown in Fig. 3. The rocket engines had the same throat area but different throat to exit area ratios, 8 to 1 and 25 to 1. The oxygen/RP-1 propellant combination was used in both rocket engines, whereas the oxygen/hydrogen combination was used only in an 8 to 1 area ratio engine. Rocket engine injector patterns are shown in Fig. 4.

2.3 MODELS AND MODEL STRUTS

In Fig. 5 are presented the dimensions of the test models. Both models have ogive forebodies and cylindrical afterbodies. As shown in Fig. 3, the 25 to 1 area ratio rocket engine was housed within the shell of the model afterbody to maintain the proper model base to rocket engine exit diameter ratio. The test installation of the 8 to 1 area ratio rocket engine is shown in Fig. 6.

The model support struts were made in two sections. The lower section was common to both models. Two upper sections, one for each rocket engine exit size, were used. The models and upper strut were made to scale with the rocket engine exit diameter.

2.4 QUENCH SYSTEM

The quench liquid (RP-1) was stored in three five-gallon high pressure vessels manifolded together. The system was remotely pressurized and regulated from the control room. The quench injector is shown in Fig. 7. The injector consisted of a series of 20 orifices, 0.025 inch in diameter, in a circular manifold mounted concentric with and just downstream of the rocket motor exit. The RP-1 was injected normal to the rocket exhaust. The injector screwed onto the body of the 8 to 1 area ratio rocket engine.

3.0 INSTRUMENTATION

All instrumentation was located in temperature-controlled boxes in the tunnel walls as shown in Fig. 8.

3.1 RADIOMETERS

Two radiometers, located in the top wall of the tunnel and equipped with plane mirrors, were used to map the infrared level of rocket plumes. The mirrors were remotely controlled to rotate about two mutually perpendicular axes. This installation permitted an axial scan of six-feet downstream and upstream of the center position of the radiometer and a unidirectional radial scan of two feet from the centerline of the tunnel. The scanning mirror position was determined by measuring the voltages across two, ten-turn potentiometers that were coupled to the scanning motors.

The radiation from the rocket exhaust plume was reflected from the scanning mirror through a quartz lens. The transmission of the quartz was greater than 80 percent from 0.26 to 3.0 microns. The reflected radiation was mechanically chopped at 750 cps and passed through an interference filter onto a lead sulfide detector. The filter, which has a peak at 2.645 microns, permitted only a band of 0.11 micron to fall on the detector. The interference filter transmittance curve is shown in Fig. 9. The 750-cps signal was amplified by a factor of 5,000. It was then recorded on magnetic tape and monitored on an oscilloscope. This same installation was also used during the rocket plume quenching program. One of the radiometers used for these programs is shown in Fig. 10.

3.2 PHOTOGRAPHIC COVERAGE

Photographic coverage included 35-mm cameras using Tri-x film with a sensitivity between 0.36 and 0.65 micron (visible light range). Movie coverage was provided with three 16-mm cameras.

3.3 PRESSURE INSTRUMENTATION

Pressure transducers were used to monitor rocket chamber pressure, and their outputs were recorded on magnetic tape.

4.0 DATA ACCURACY

Table 1 presents the estimates of the error in tunnel parameters and data variables. The uncertainties were estimated from a study of the measuring equipment and the results obtained during the tunnel

operation for a probability of 95 percent. The maximum variation in centerline Mach number is ±0.02, and the off-centerline Mach number agrees with centerline Mach numbers within ±0.01. A more extensive discussion of the uncertainties in the tunnel flow parameters is presented in Ref. 3.

5.0 PROCEDURE

5.1 CALIBRATIONS

The radiometer position indicators were calibrated by focusing the radiometers on an infrared source at measured tunnel stations. Indicator output versus position was then plotted. Calibrations were made first along the rocket engine centerline for rocket plume axial position and then along lines perpendicular to the tunnel centerline for the rocket plume radial position.

Spectral radiance calibrations of the radiometer were made at sea-level conditions using two blackbody sources operating in the infrared region of the electromagnetic wave spectrum. The calibrations were performed in the tunnel by placing each source in such a way that the radiometer viewed the central portion of the source. One source provided temperatures up to 230°C and was used for the low radiance levels. A variable aperture on the second source provided varying degrees of spectral radiance at the radiometer. This calibration source temperature was approximately 660°C. No attempt was made to correct the data for the difference in absorbtivity of the air at the various test conditions. However, it is estimated that the absorbtivity of air decreased approximately nine percent between sea level and the maximum test altitude for an optical path length of 12 ft.

5.2 TESTS

When tunnel conditions were established, a firing countdown was initiated, and during the ensuing countdown, test monitoring instrumentation equipment and propellant system controls were activated.

Test data were obtained at the test conditions shown in Table 2. The 8 to 1 nozzle-exit area ratio rocket engine using oxygen/RP-1 propellant was investigated at static sea-level conditions and at Mach numbers of 1.75 and 2.15 at pressure altitudes of 50,000 and 66,500 ft, respectively. The 8 to 1 nozzle-exit area ratio rocket engine using

oxygen/hydrogen propellant was investigated only at static sea-level conditions. The 25 to 1 nozzle-exit area ratio rocket engine was investigated for only the oxygen/RP-1 propellant combination and for Mach numbers of 1.75 and 2.60 at pressure altitudes of 50,000 and 83,000 feet, respectively.

For the major portion of the test, the equivalence ratio for RP-1 firings was approximately 1.5. Several RP-1 firings were made with equivalence ratios of 1.1 and 1.9 with the 8 to 1 area ratio engine. An equivalence ratio of 2.0 was maintained for all hydrogen firings. The equivalence ratios presented in this report are the average equivalance ratio for each rocket firing because a constant equivalence ratio could not be maintained during the long rocket firing time (100 to 5000 sec).

After steady-state operation was attained, the procedure varied with the test phase.

a. Mapping Phase. Radial scans of the rocket plume were made with two radiometers at axial increments of ten inches from the rocket motor. Following the radiometer scans, several photographs were taken with the 35-mm cameras.

b. Quenching Phase. The quenching liquid (RP-1) was injected at an increasing rate until an optimum condition was reached. The optimum condition was determined by monitoring the radiometer outputs on an oscilloscope. When the radiation level was minimized, an axial scan of the plume centerline was made with two radiometers. Figure 11 is a block diagram of the quenching system instrumentation.

6.0 RESULTS AND DISCUSSION

6.1 MAPPING PHASE

The size of the radiometer field of view had an appreciable effect upon the resultant data. Shown in Fig. 12 are raw data curves of radial scans of the plume for both radiometers. The upstream radiometer with a field of view one fourth that of the downstream radiometer gives the more accurate measurement for the local value of spectral radiance. The slopes of the curves shown in Fig. 12 indicate the relative sensitivity of the two instruments to the change in radiation level along the plume radius.

The infrared radiation levels along the plume axis at the three test trajectory conditions for the 8 to 1 area ratio rocket engine are presented in Fig. 13 for an equivalence ratio of approximately 1.5. There is no significant difference in radiation level for the two tunnel air-on test conditions. The radiation level at the static sea-level conditions is considerably lower than the tunnel air-on conditions. The reasons for this large difference are not understood, especially because only a small portion of the difference in radiation level is caused by atmospheric absorption.

The infrared radiation distribution for the three test trajectory conditions with the 8 to 1 area ratio rocket engine are presented in Figs. 14, 15, and 16. For the purpose of presenting curves indicative of the radiation profiles, the minimum spectral radiance levels were selected as 0.010 for the upstream radiometer and 0.020 for the downstream radiometer. This selection was governed by the background radiation level with the rocket firing indicated by the radial scans of the rocket plume (see Fig. 12 for typical radial scans). The spreading of the radiating portion of the plume remained approximately the same for the two tunnel air-on test conditions. Greater spreading would be expected at the higher altitude; however, the increase in Mach number apparently counteracts this effect.

The effect of equivalence ratio on the infrared radiation level along the rocket plume axis is shown in Fig. 17 for approximate equivalence ratios of 1.1, 1.5, and 1.9 at static sea-level conditions. The highest equivalence ratio produced the highest radiation level. It is evident that the higher equivalence ratios provide excess fuel for burning in the rocket plume and that the chemiluminescent processes accompanying the afterburning are responsible for the differences in the radiation levels. There is a leveling off of the radiation level as the stoichiometric condition is approached. Radial scans at an axial position 30-in. ($x/r_e = 40$) downstream of the rocket exit are shown in Fig. 18. The secondary peaks at approximately y/r_e values of 12 and 25 coincide with the location of a black grid painted on the tunnel floor for visual measurements. It is obvious that the spectral radiance measured beyond radial values of $y/r_e \approx 9$ is caused by plume radiation reflected from the tunnel walls.

Isoradiance and centerline radiance curves for both oxygen/hydrogen and oxygen/RP-1 propellant combinations are presented in Figs. 19 and 20. Several firings were made at static sea-level conditions using oxygen/hydrogen propellant combination with the 8 to 1 area ratio rocket engine. The equivalence ratios were approximately the same for the two combinations, $\Phi \approx 2.0$ for oxygen/hydrogen and $\Phi \approx 1.9$ for oxygen/RP-1. No

data were obtained with the upstream radiometer for the oxygen/hydrogen firing. No appreciable differences between the centerline radiance levels for the two propellant combinations were found. Furthermore, the isoradiance curves indicate a similarity in the plume radiation geometry. The large discrepancy between the readings of the upstream and downstream radiometers at $x/r_e = 107$ in Fig. 20 is attributed to the fact that the two radiometer scanning mirrors are viewing different portions of the plume. The downstream radiometer is directly above the plume at this axial location, whereas the upstream radiometer scanning mirrors must be turned through an angle of 45 deg to view the same location, thus providing an oblique "slice" of the plume to be viewed by the radiometer.

Presented in Fig. 21 is a plume photograph of the oxygen/RP-1 propellant combinations at test trajectory conditions for the 25 to 1 area ratio rocket engine and the boundary plotted from the photograph. Limited data were available to compare the temperature boundary from Ref. 1 with the visible plume boundary in Fig. 21. For the same test trajectory conditions, the temperature boundary at an $x/r_e \approx 100$ is approximately twice as large as the visible plume boundary, and the plume temperature profile indicates that the plume stagnation temperature is approximately 2000°R at the visible plume boundary. The airstream stagnation temperature was 684°R at this test condition.

6.2 QUENCHING PHASE

During the quenching phase of the test program, attempts were made to extinguish the afterburning flame by injecting liquid RP-1 peripherally into the exhaust of the rocket engine at the nozzle exit. The reduction of the plume infrared radiation is desirable to reduce the effectiveness of detection systems that measure plume infrared radiation.

During quenching, radiometer data were recorded at three test conditions. At all conditions the quenching flow rate was increased until further increases resulted in no additional reductions in the radiation level. In Figs. 22, 23, and 24 the spectral radiance along the rocket plume axis is presented for the quenched and unquenched conditions for three different test conditions. The discontinuities that appear at an x/r_e value of approximately 195 in Figs. 23 and 24 can be attributed to reflection from a rake assembly installed in the tunnel test section to measure rocket plume pressure, temperature, and gas composition. Data downstream of this interference are therefore not valid.

The absolute level of centerline spectral radiance for the quenching phase is in error for axial scan data obtained from the upstream radiometer. The axial scanning mirrors of the radiometer were found to be scanning at an angle off the plume centerline. Because only axial scans were taken during the quenching phase, the spectral radiance values obtained will not necessarily agree with the radial scan spectral radiance values presented in the mapping phase for the upstream radiometer at the same test conditions. The relative values, however, for the quenched and unquenched conditions are valid.

At all test conditions both the radiation level at the filtered wavelength and the visible flame were considerably reduced by the quenching fluid. The visible flame appeared to be more completely quenched for the two tunnel air-on conditions. Quenching had the least effect upon the radiation level at the highest Mach number, but the radiation levels were so low as to make such a conclusion questionable. Even though the quenching flow was least for this condition, increases in the quenching flow did not reduce the radiation level. This result is attributed to the fact that the thickness of the mixing layer between the rocket exhaust and the free stream decreases with increasing Mach number. The quenching fluid affects primarily the mixing layer and not the central core; consequently, less quenching fluid is required where peripheral burning is or may be, marginal and dependent upon oxygen from the free stream. Because the mixing layer was largest at zero Mach number and more oxygen from the surrounding medium was available, more fluid was required for quenching.

It is important to note that the radiation level is presented for only a small wavelength band centered at 2.645 microns with a bandwidth of approximately 0.11 micron. The effect over the complete infrared bandwidth therefore is not known. The spectral radiance of rocket exhaust plumes over the complete infrared band of the spectrum is presented in Refs. 4 and 5.

7.0 CONCLUSIONS

Rocket engines using oxygen/RP-1 propellants were used to generate an exhaust plume for infrared radiation studies. Tests at static sea-level conditions included a variation of equivalence ratio and nozzle-exit area ratio. At several Mach number and pressure altitude conditions, two nozzle-exit area ratios were used. A similar rocket engine using oxygen/hydrogen as propellants was used at static sea-level conditions and for one equivalence ratio. Infrared radiation surveys of the

rocket engine plumes taken at a wavelength of 2.645 microns with a 0.11-micron bandwidth resulted in the following conclusions:

1. The infrared radiation levels at Mach number and altitude conditions were found to be significantly higher than those at static sea-level conditions for approximately the same equivalence ratio.
2. The infrared radiation level of the rocket plume increased with increasing fuel richness for the oxygen/RP-1 propellants at static sea-level conditions.
3. The infrared radiation levels along the rocket plume axis for static sea-level conditions were approximately the same for the oxygen/RP-1 and oxygen/hydrogen propellants at approximately the same equivalence ratio.
4. The peripheral injection of quenching fluid (RP-1) in a direction normal to the rocket exhaust reduced the visible rocket plume and the plume infrared radiation for the oxygen/RP-1 propellant rocket engine. (Only the 8 to 1 area ratio, oxygen/RP-1 propellant rocket engine was used in the quenching phase of the test.)
5. The quenching effect was found to decrease with increasing Mach number and altitude for constant equivalence ratio.

REFERENCES

1. Gerke, P. D. "Characteristics of Rocket Engine Plumes in Supersonic Flow." AEDC-TDR-62-98, July 1962.
2. Test Facilities Handbook, (4th Edition). "Propulsion Wind Tunnel Facility, Vol. 3." Arnold Engineering Development Center, July 1962.
3. Nichols, J. H., Davis, M. W., Garner, C. L. "Initial Aerodynamic Calibration Results for the AEDC-PWT 16-Foot Supersonic Tunnel." AEDC-TDR-62-55, March 1962.
4. Sutton, J. W. "Laboratory Studies of Rocket Plume Radiation at Reduced Pressure." AFCRL-62-235 (AD273435), December 1961.
5. Briscoe, R. D., Bullara, L. A. "Infrared Spectra from Titan, Polaris and Liquid-Hydrogen Motors." Proceedings of Infrared Information Symposia, Office of Naval Research, Vol. 5, No. 3, July 1960. (SECRET)

TABLE 1

PRECISION OF MEASUREMENTS

Parameter		Δ Error
M_∞		±0.02
N_λ		±0.003
Z		±720
x/r_e	Isoradiance Curves	
	8 to 1 Rocket Engine	±0.13
	25 to 1 Rocket Engine	±0.08
x/r_e	Photographic Boundaries	
	25 to 1 Rocket Engine	±0.37
y/r_e	Isoradiance Curves	
	8 to 1 Rocket Engine	±0.13
	25 to 1 Rocket Engine	±0.08
y/r_e	Photographic Boundaries	
	25 to 1 Rocket Engine	±0.37
Φ	(O_2/RP-1) during a Rocket Firing	±0.1
Φ	(O_2/H_2) during a Rocket Firing	±0.1

TABLE 2
TEST CONDITIONS

Rocket Engine Area Ratio	Propellant Combination	M_∞	Z, ft	T_{t_∞}, °R
8 to 1	O_2/RP-1	0	sea level	610
8 to 1	O_2/RP-1	1.75	50,000	687
8 to 1	O_2/RP-1	2.15	66,500	717
8 to 1	O_2/RP-1	0	sea level	518
25 to 1	O_2/RP-1	1.75	50,000	675
25 to 1	O_2/RP-1	2.60	83,000	802
25 to 1	O_2/RP-1	2.60	83,000	854
25 to 1	O_2/RP-1	2.60	83,000	880
8 to 1	O_2/H_2	0	sea level	522

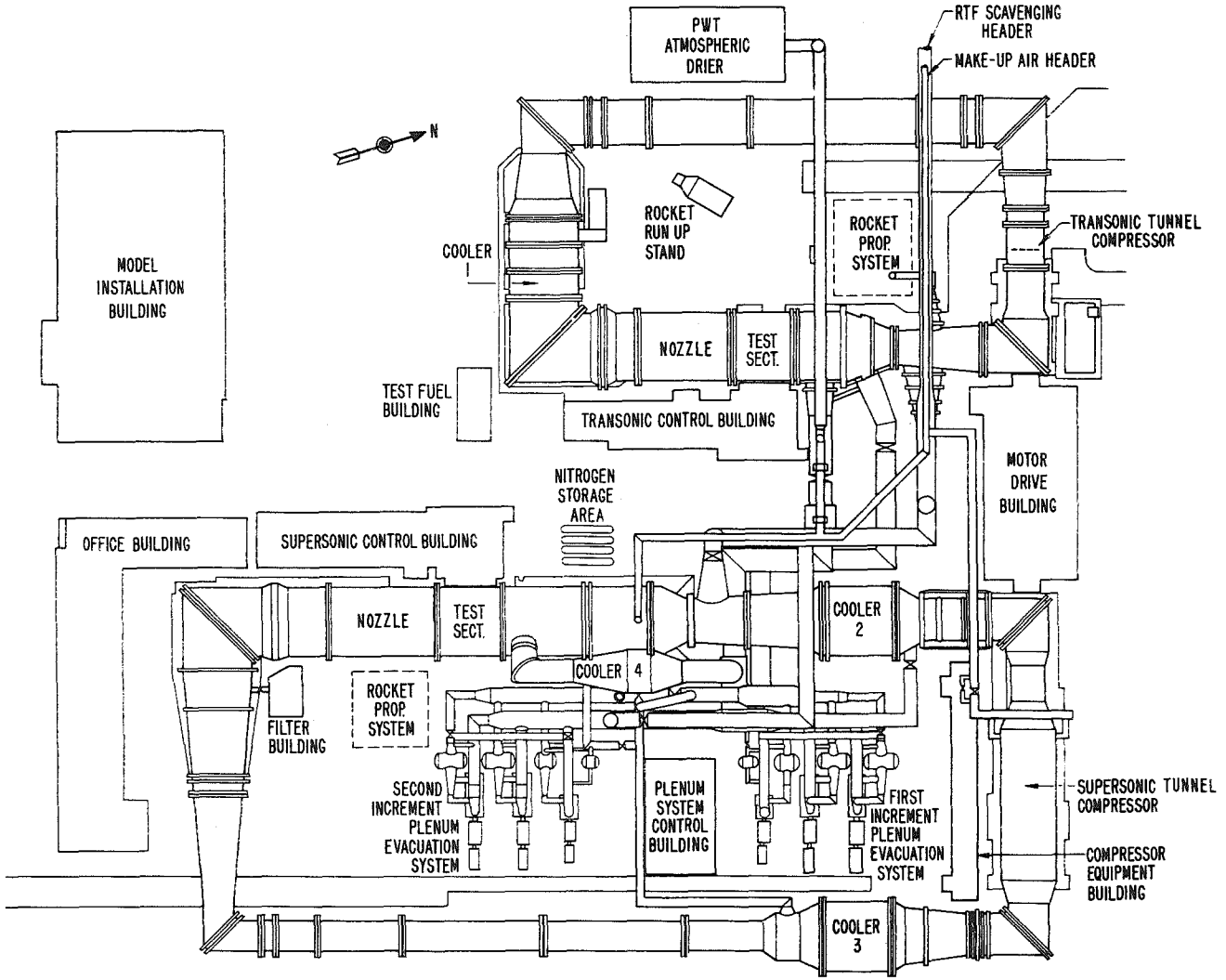

Fig. 1 The PWT 16-Ft Supersonic Tunnel and Associated Support Equipment

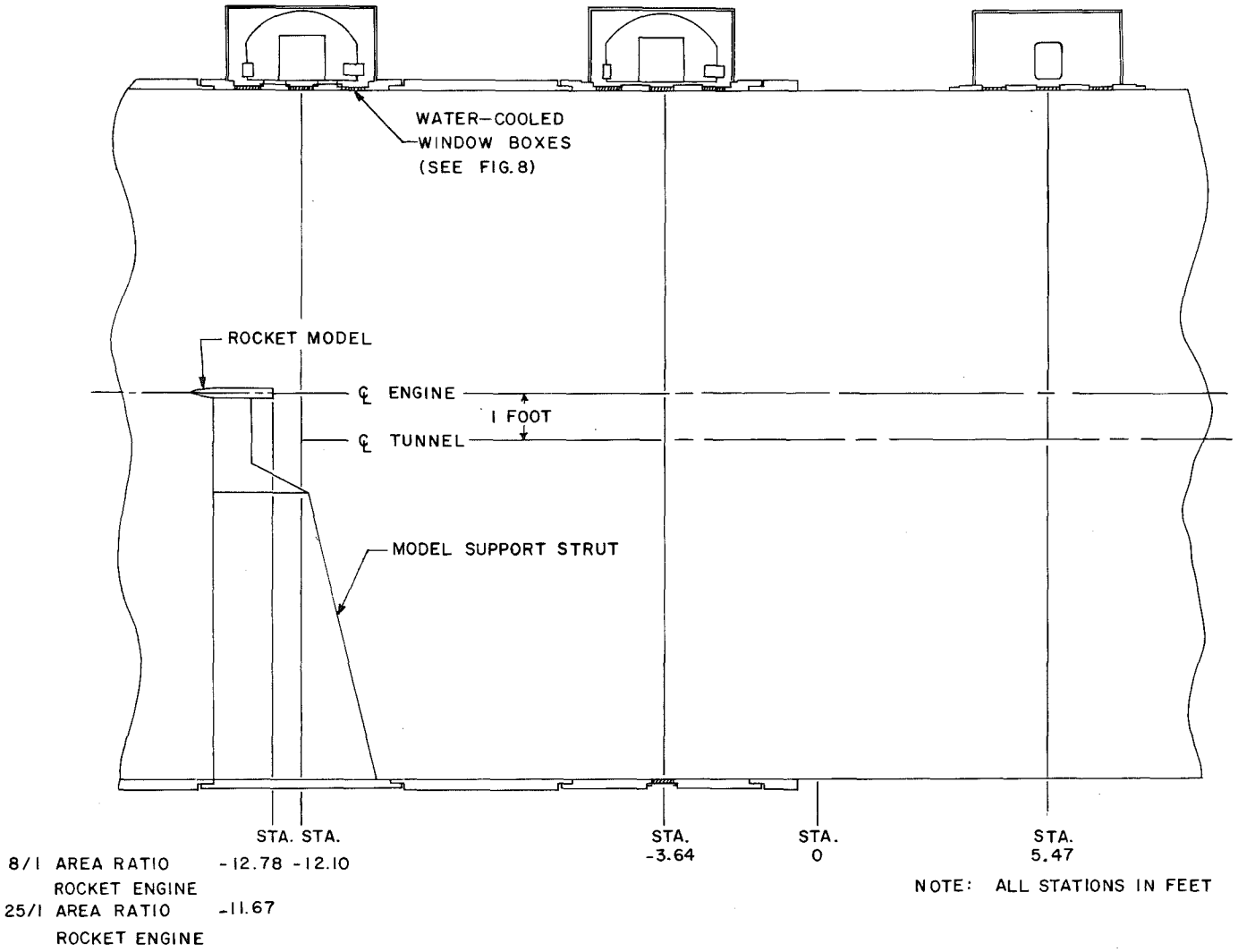

Fig. 2 Location of Test Equipment in PWT 16-Ft Supersonic Tunnel

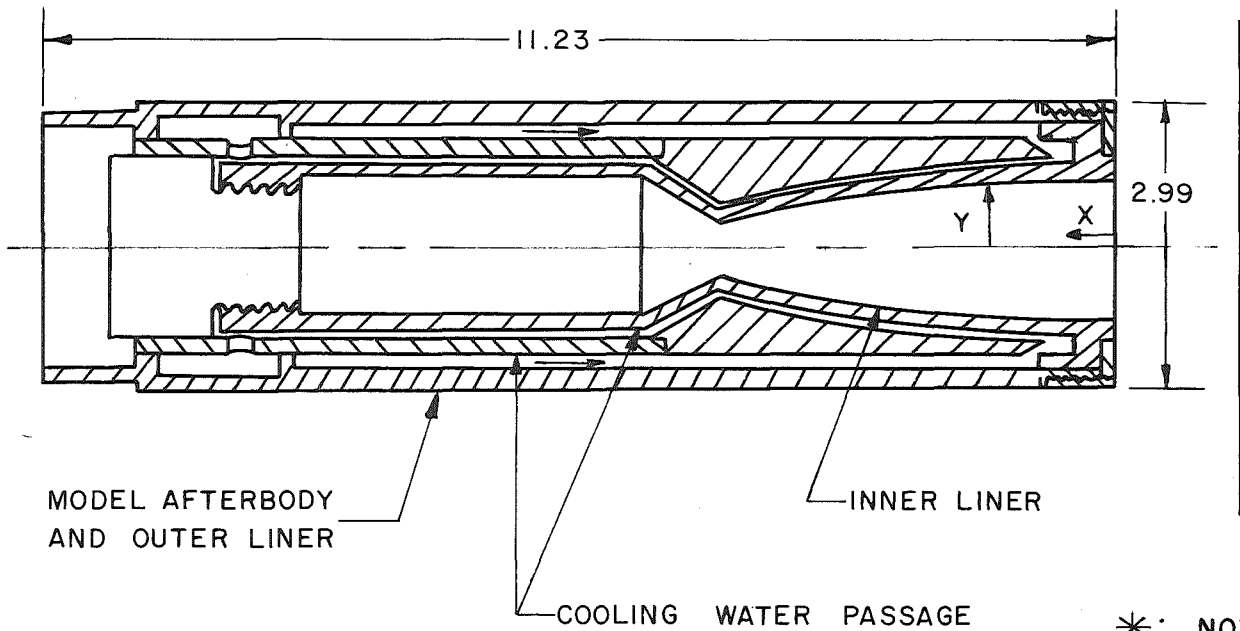

NOZZLE COORDINATES

X	Y
0	.758
.822	.722
1.548	.678
2.130	.629
2.454	.595
2.737	.560
2.983	.523
3.199	.485
3.387	.446
3.550	.406
3.662	.375
*4.069	.268

*: NOZZLE THROAT COORDINATES

NOTE: ALL DIMENSIONS IN INCHES

a. 8 to 1 Area Ratio Rocket Engine

Fig. 3 Rocket Engine Details

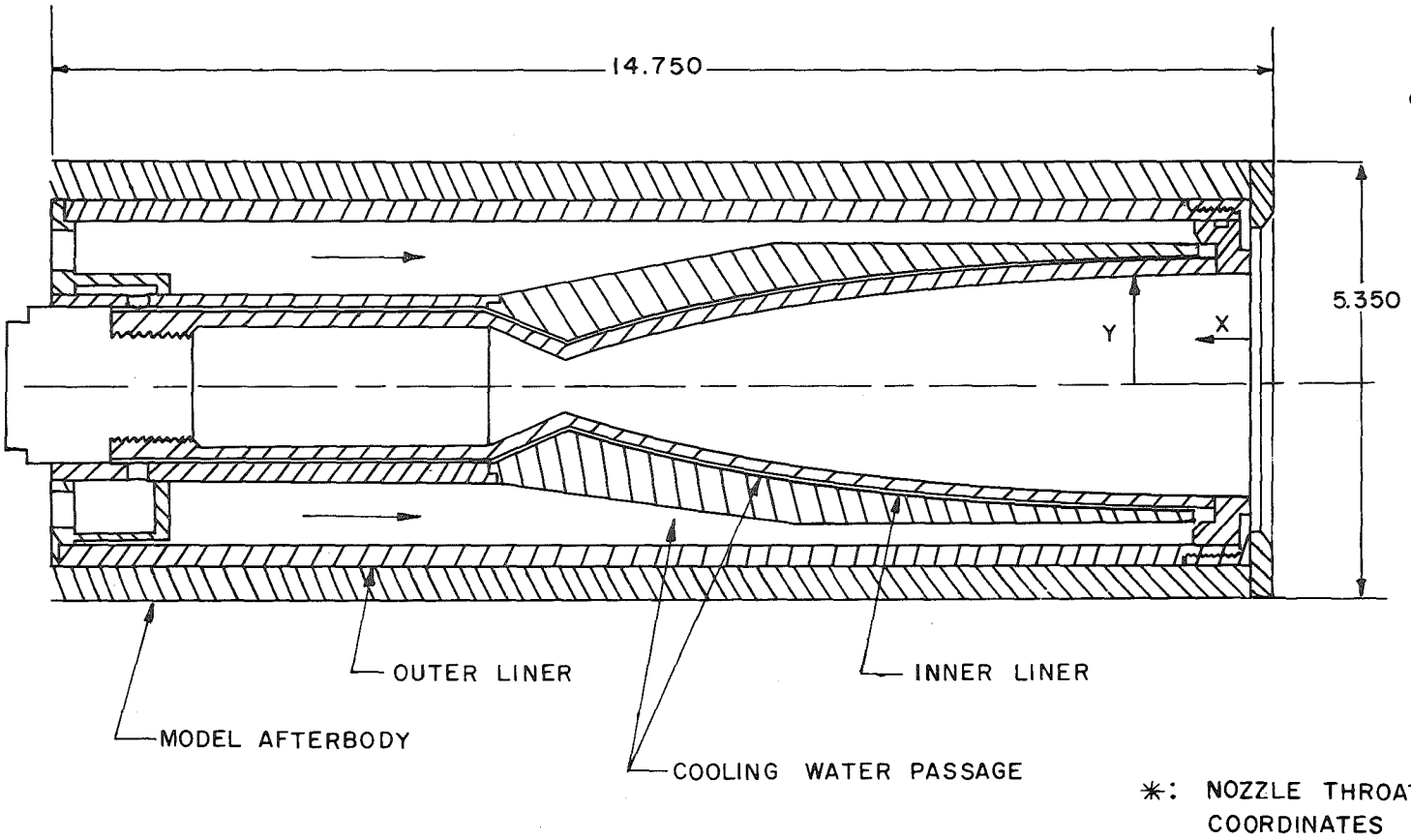

NOZZLE COORDINATES

X	Y
0	1.339
.343	1.326
.881	1.302
1.843	1.245
2.274	1.229
3.051	1.177
3.730	1.124
4.848	1.014
5.718	.901
6.398	.787
6.931	.676
7.347	.566
7.671	.460
7.727	.438
*8.238	.268

*: NOZZLE THROAT COORDINATES

NOTE: ALL DIMENSIONS IN INCHES

b. 25 to 1 Area Ratio Rocket Engine

Fig. 3 Concluded

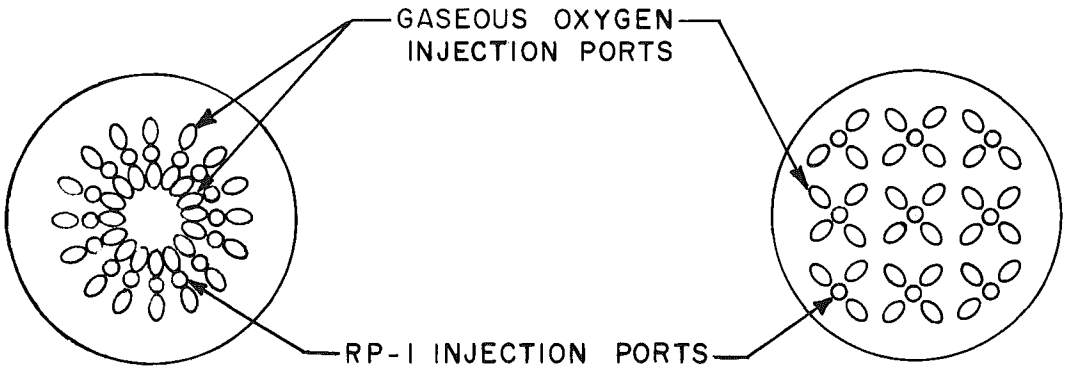

a. O_2/RP-1 Propellant Injectors

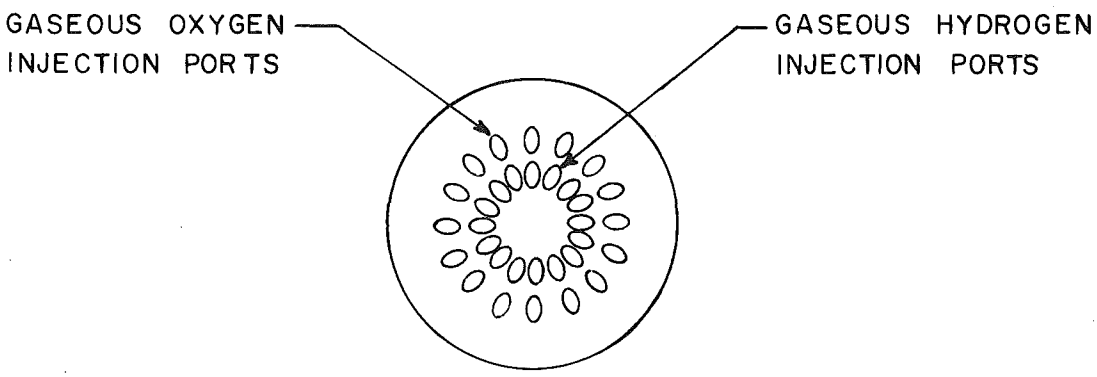

b. O_2/H_2 Propellant Injector

Fig. 4 Rocket Engine Injectors

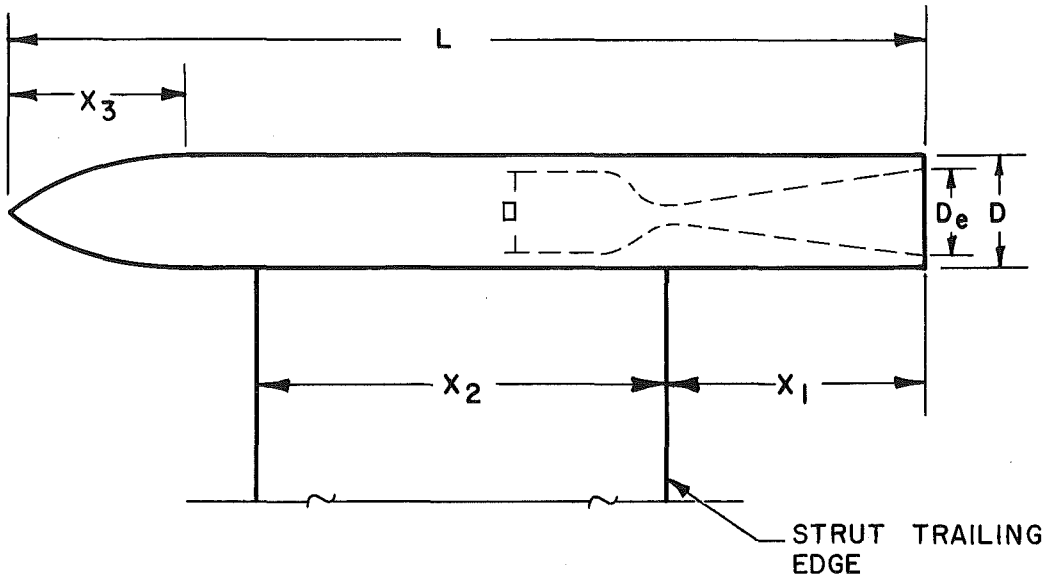

ENGINE AREA RATIO	L	D	D_e	X_1	X_2	X_3
8 : 1	24.00	2.99	1.52	6.70	10.60	6.00
25 : 1	42.85	5.35	2.68	11.96	18.92	10.72

NOTE: ALL DIMENSIONS IN INCHES

Fig. 5 Model Dimensions

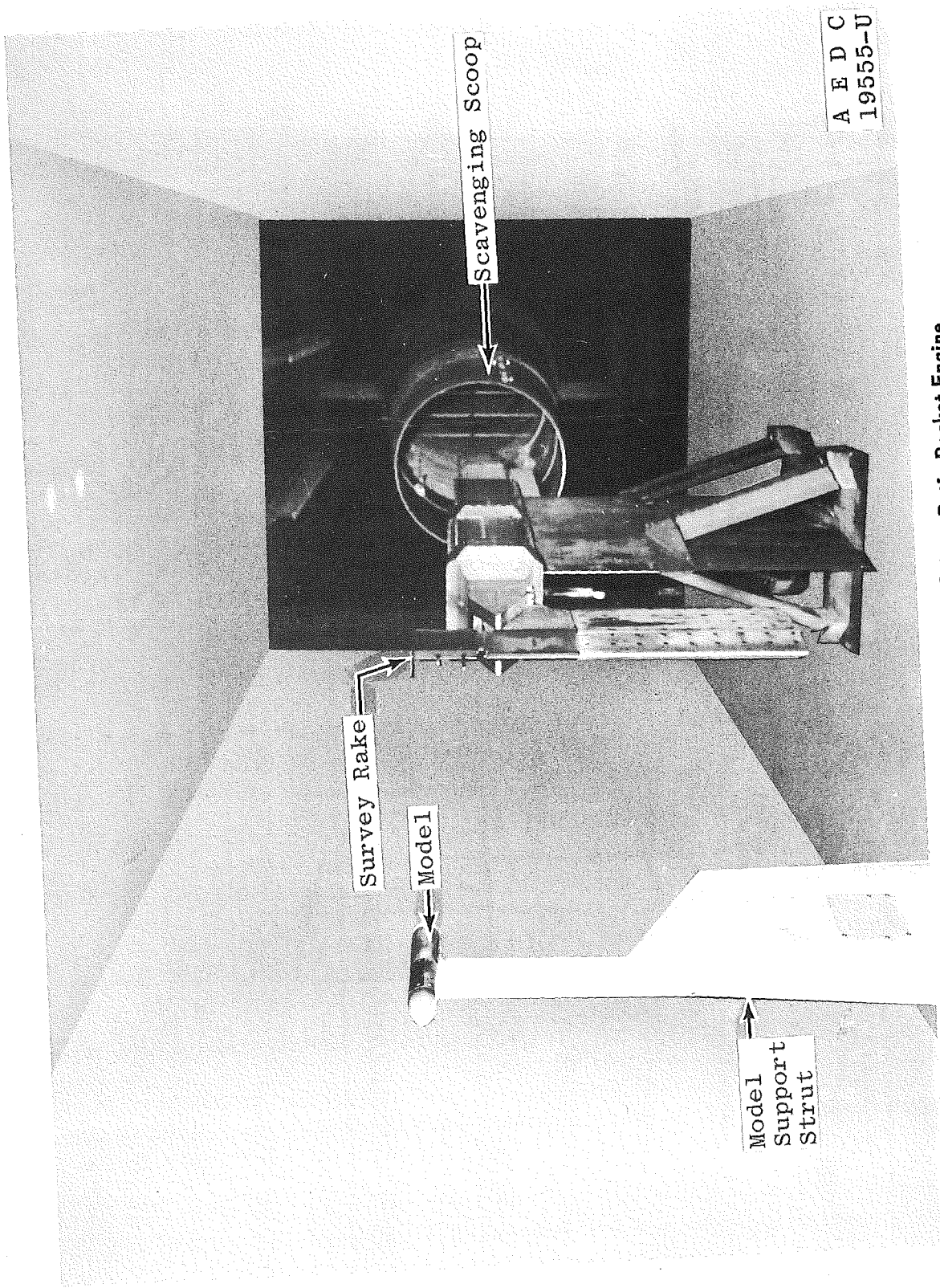

Fig. 6 Test Installation of 8 to 1 Area Ratio Rocket Engine

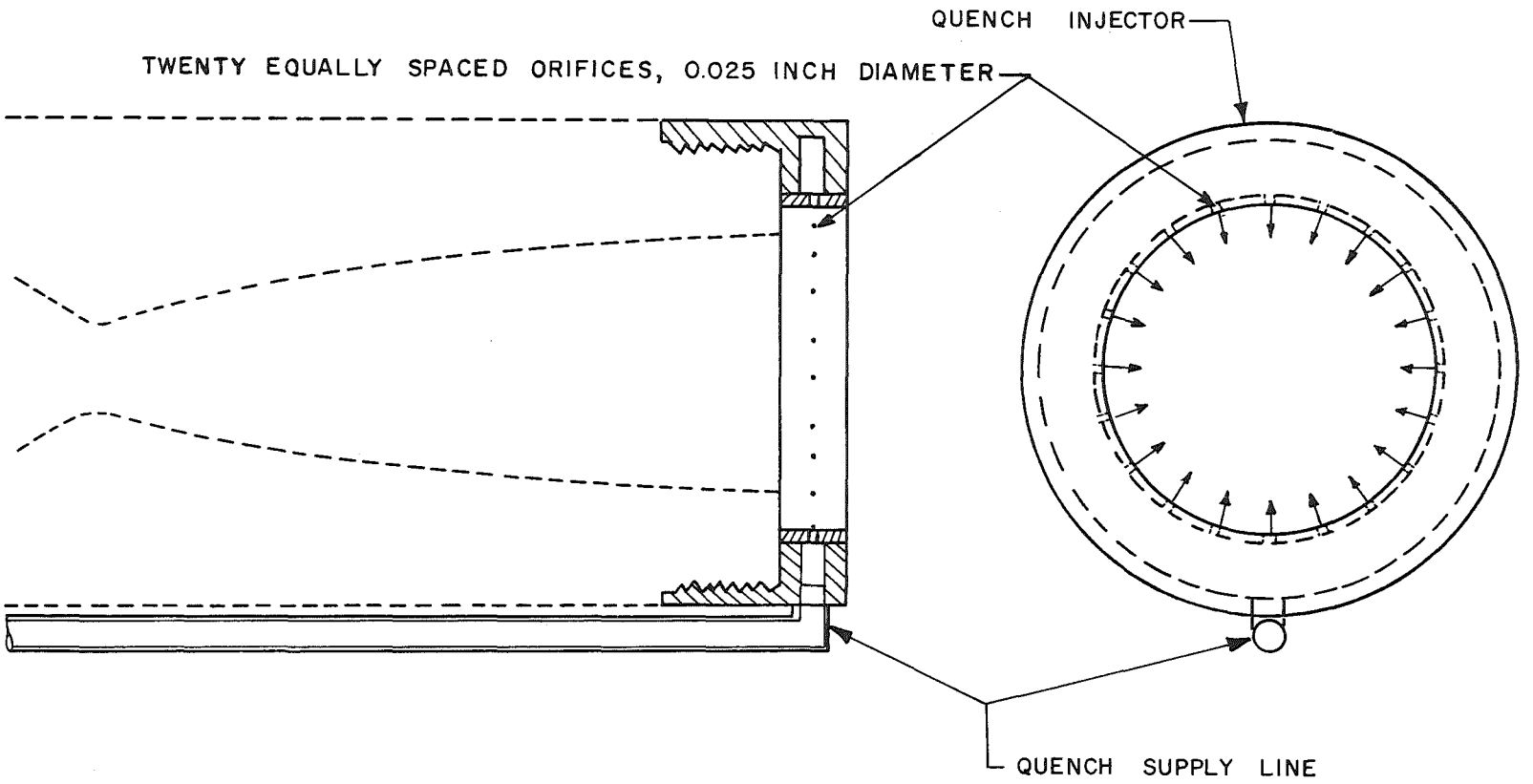

Fig. 7 Rocket Engine Quench Injector

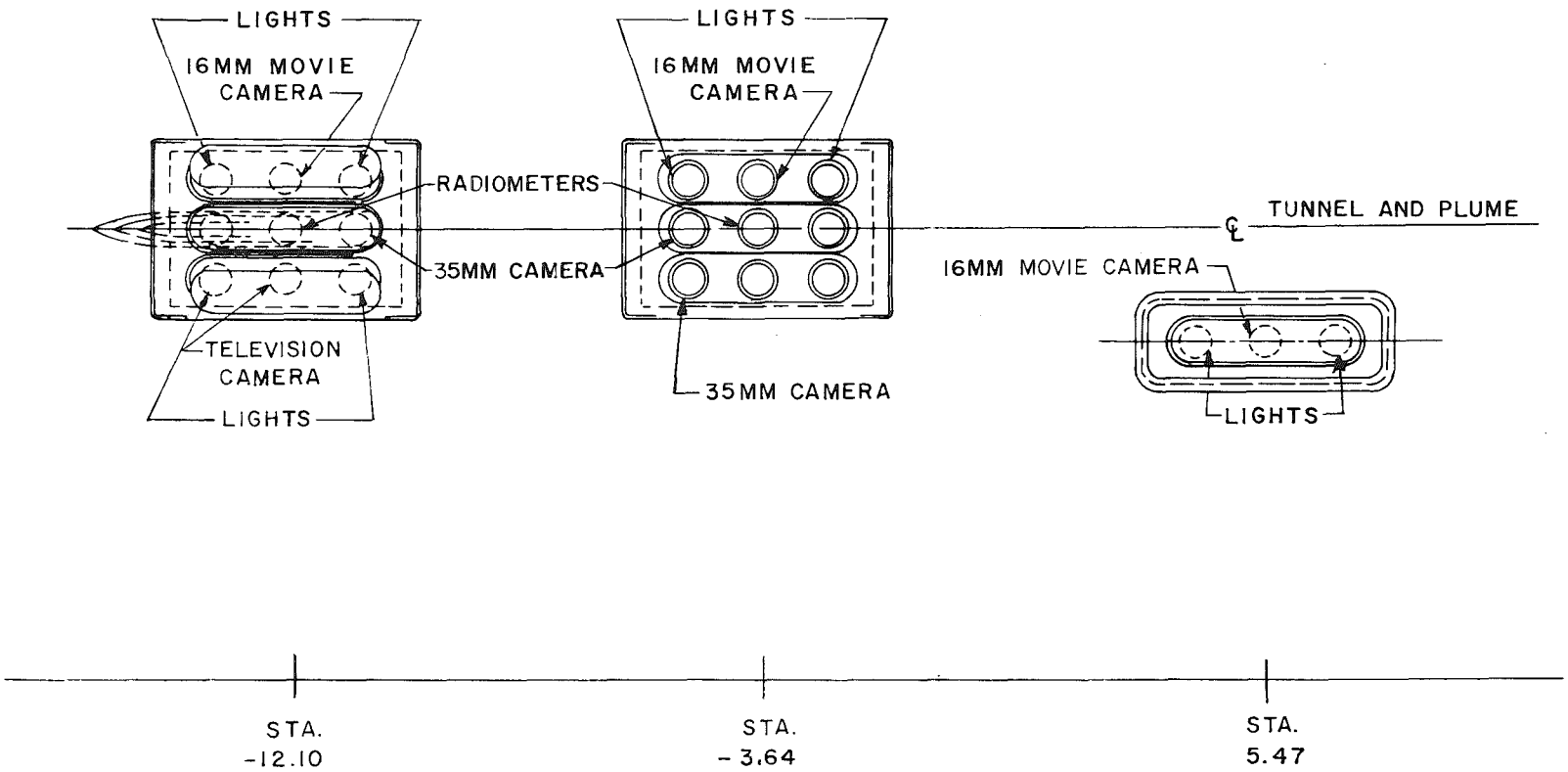

Fig. 8 Mapping and Quenching Phases Instrumentation Location (Top Wall)

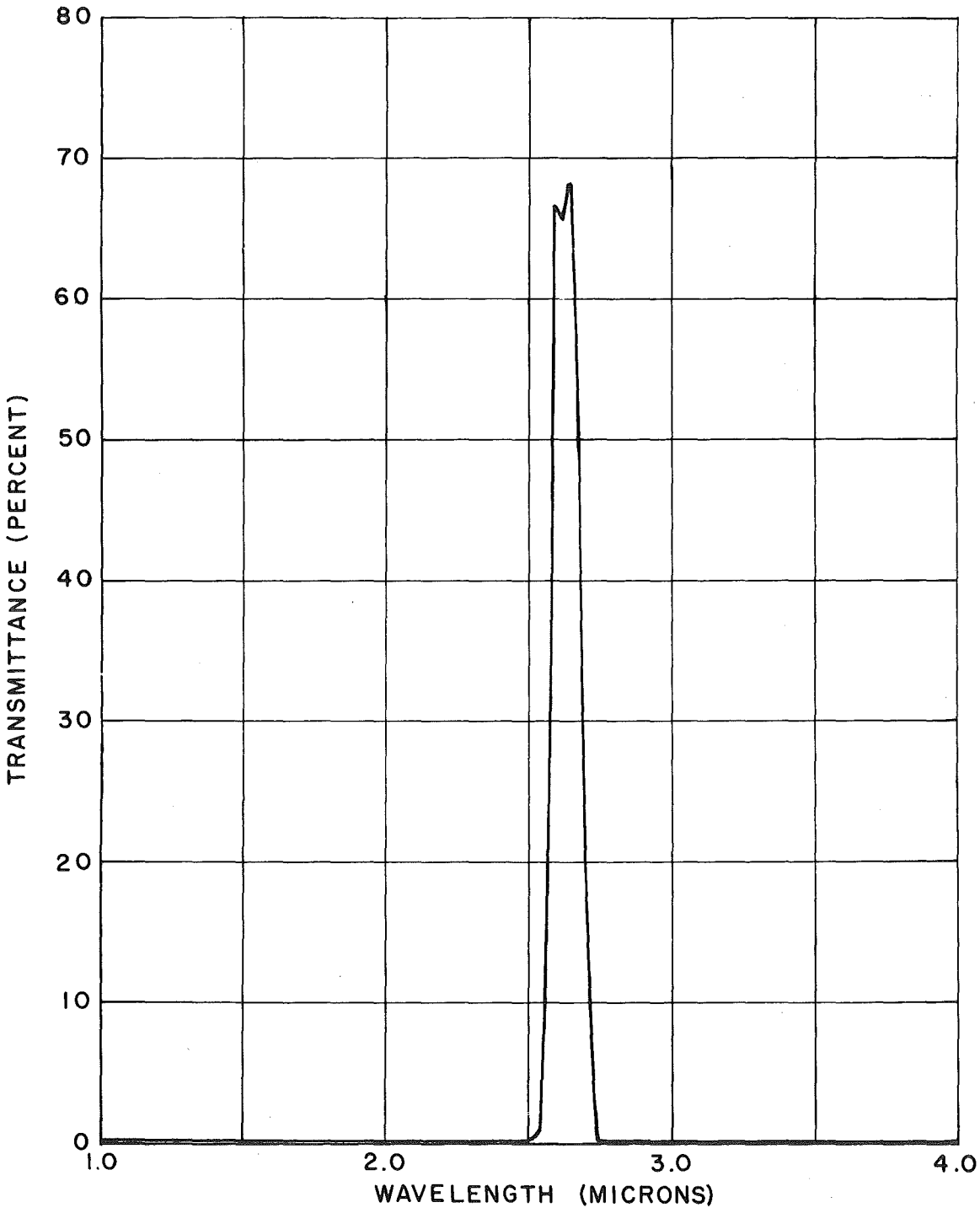

Fig. 9 Transmittance of the 2.645-micron Bandpass Filter

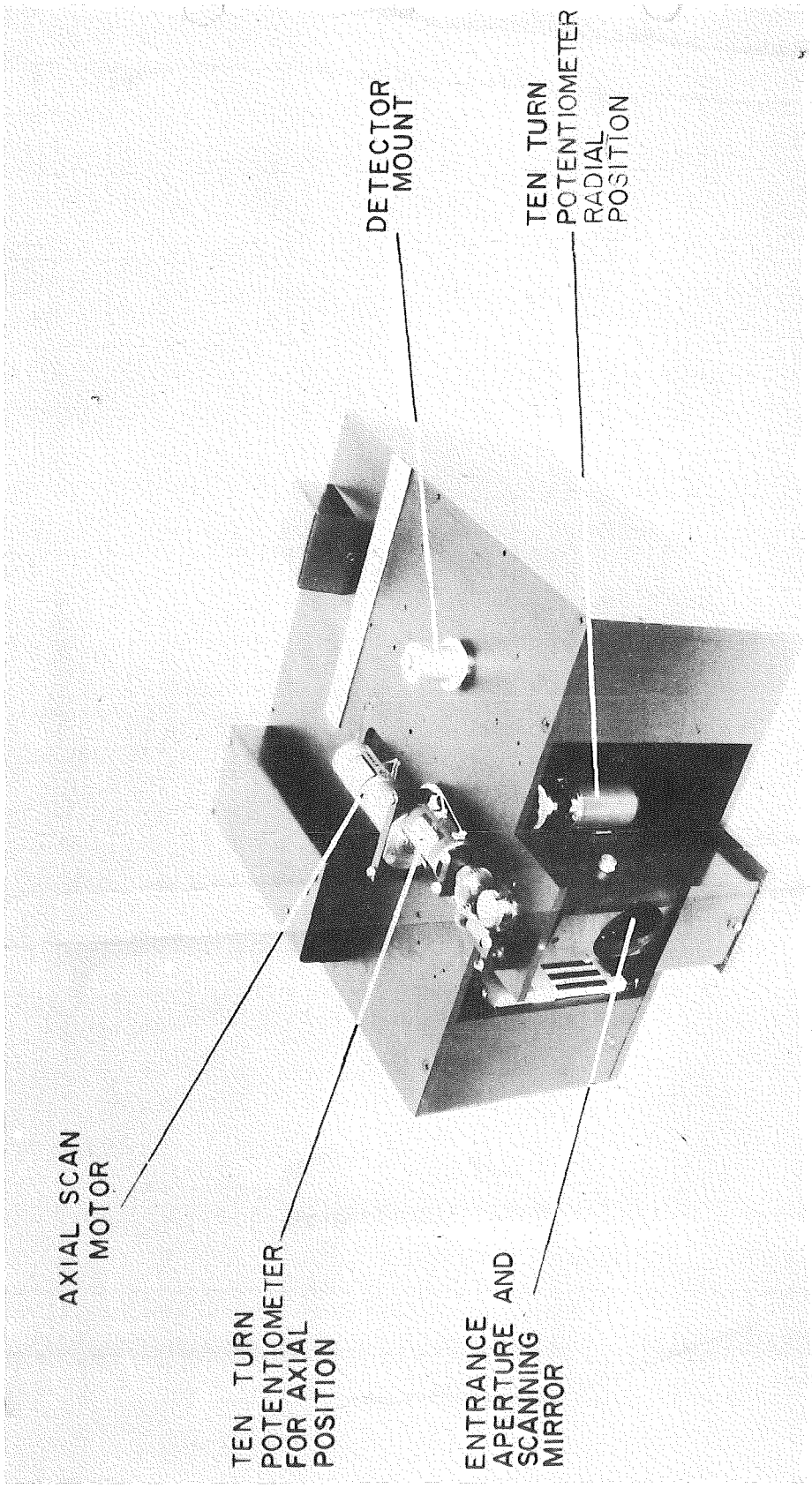

Fig. 10 Photograph of Infrared Scanning Radiometer

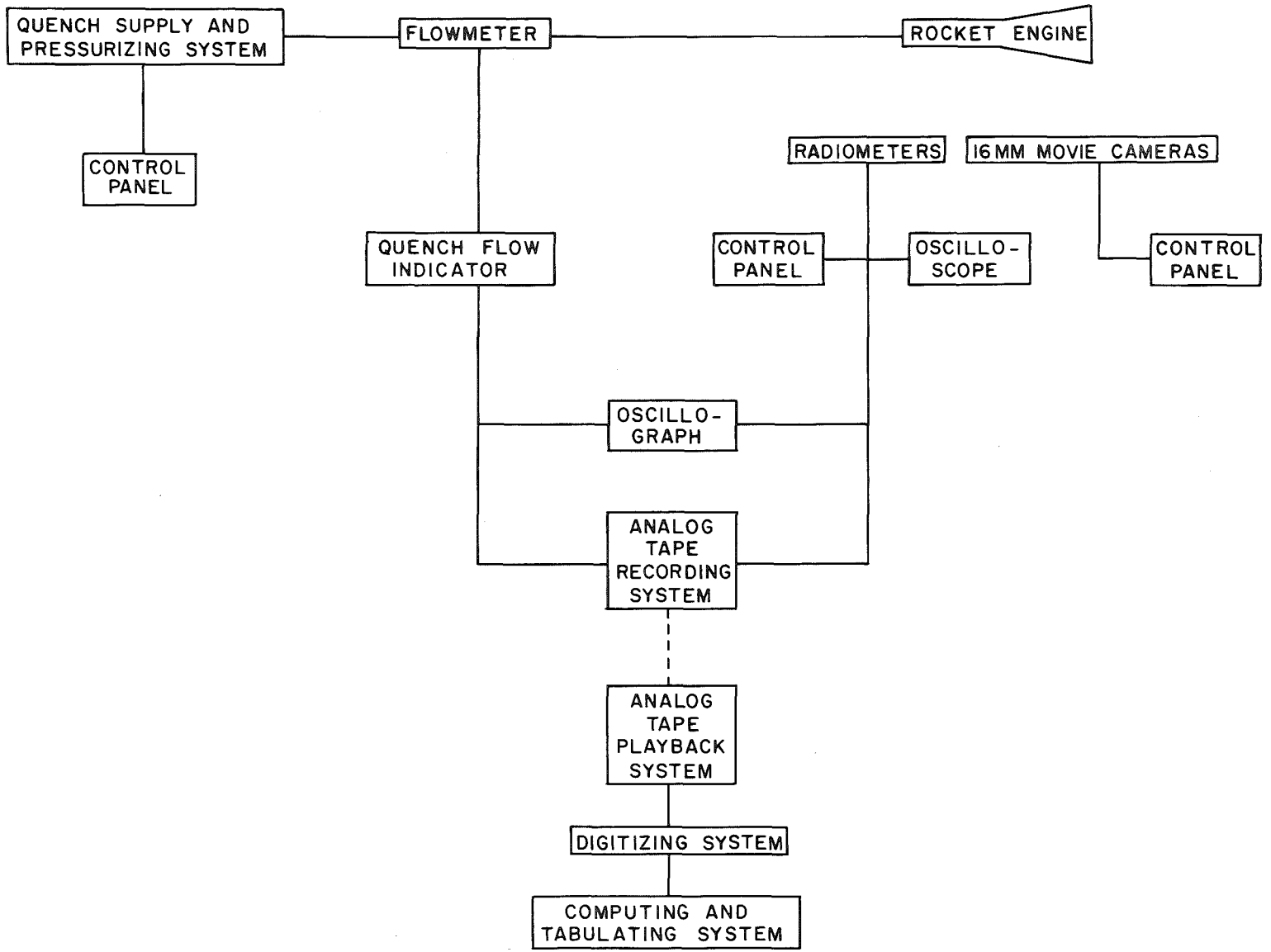

Fig. 11 Quench System Instrumentation

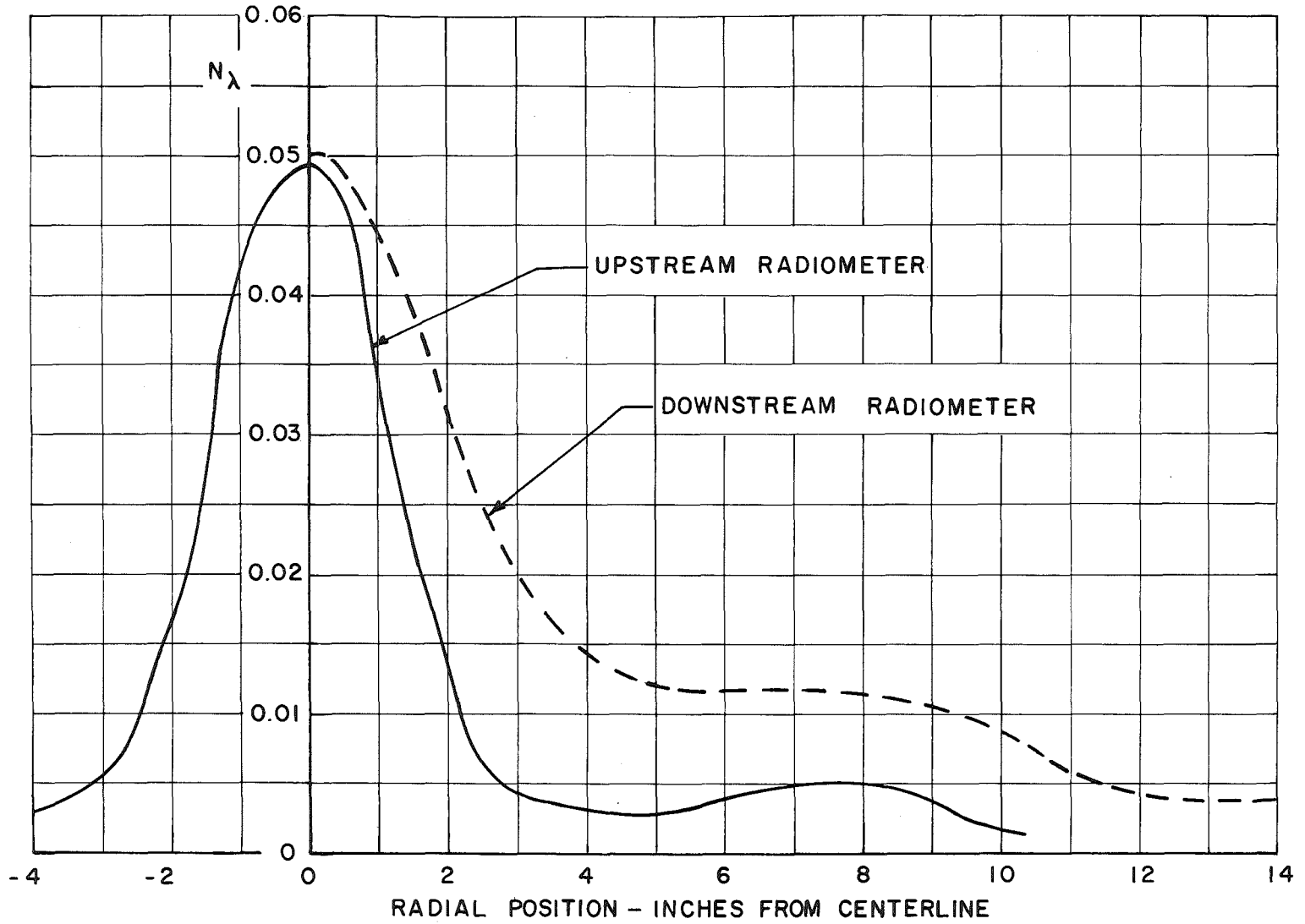

Fig. 12 Typical Radiometer Radial Scan Data, x = 80 in.

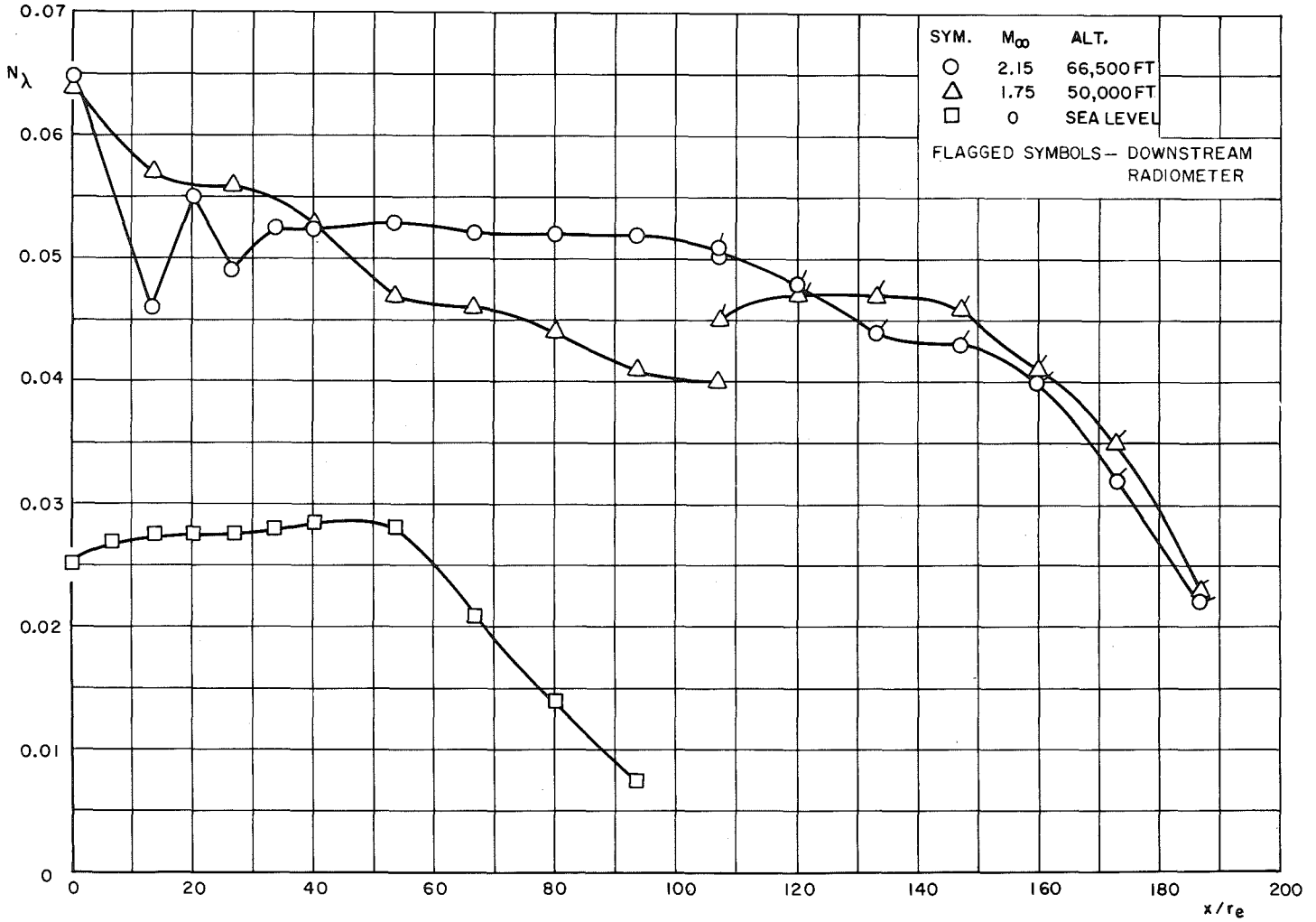

Fig. 13 Comparison of Rocket Engine Plume Centerline Spectral Radiance for Different Test Trajectory Conditions, 8 to 1 Area Ratio Rocket Engine, Oxygen/RP-1 Propellants, $\Phi \approx 1.5$

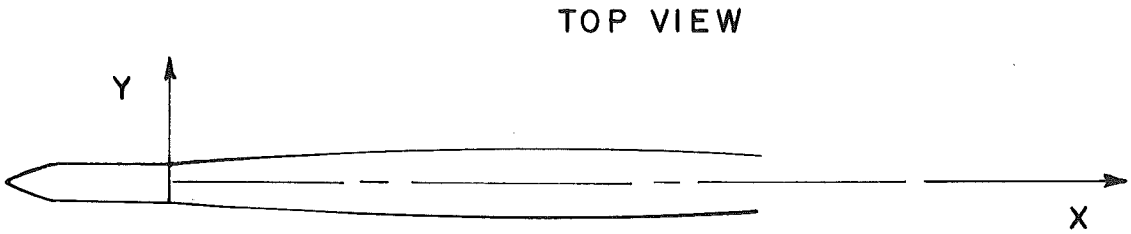

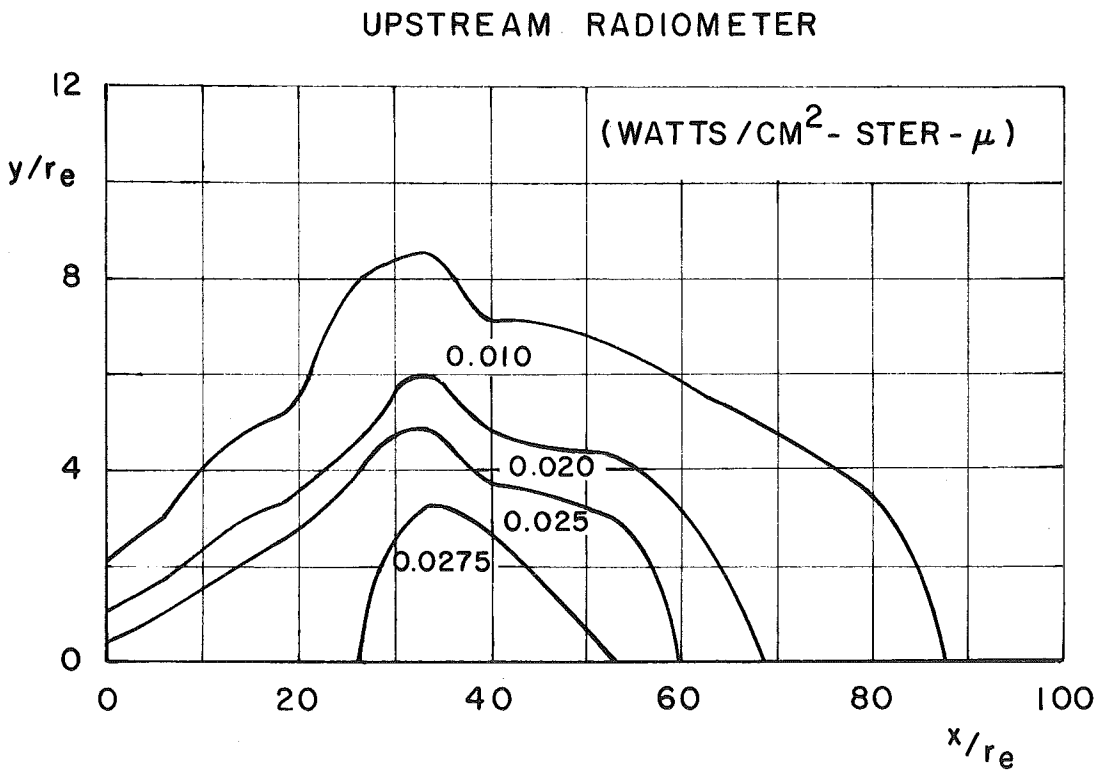

Fig. 14 Isoradiance Curves for the 8 to 1 Area Ratio Rocket Engine, Oxygen/RP-1 Propellants, $\Phi \approx 1.5$, $M_\infty = 0$, Sea Level

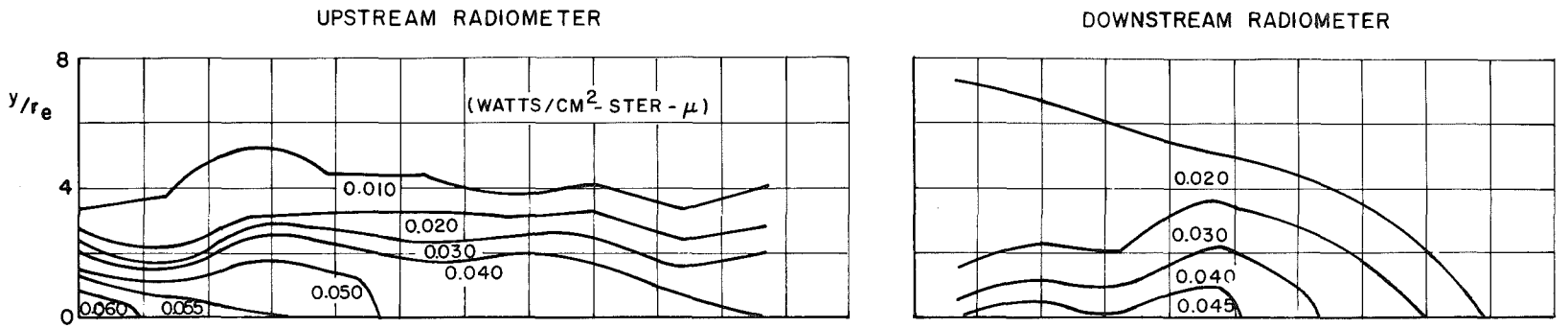

Fig. 15 Isoradiance Curves for the 8 to 1 Area Ratio Rocket Engine, Oxygen/RP Propellants, $\Phi \approx 1.5$, $M_\infty = 1.75$, Z = 50,000 ft

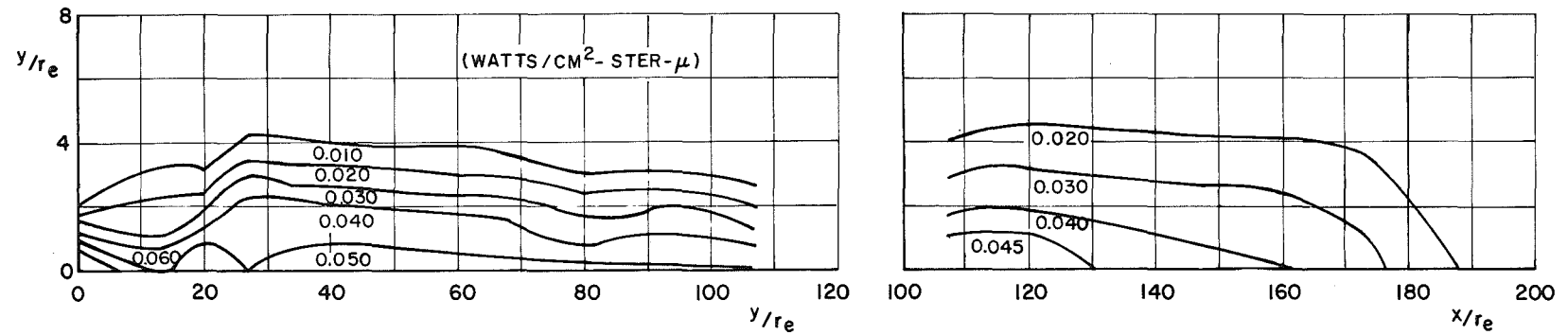

Fig. 16 Isoradiance Curves for the 8 to 1 Area Ratio Rocket Engine, Oxygen/RP-1 Propellants, $\Phi \approx 1.5$, $M_\infty = 2.15$, Z = 66,500 ft

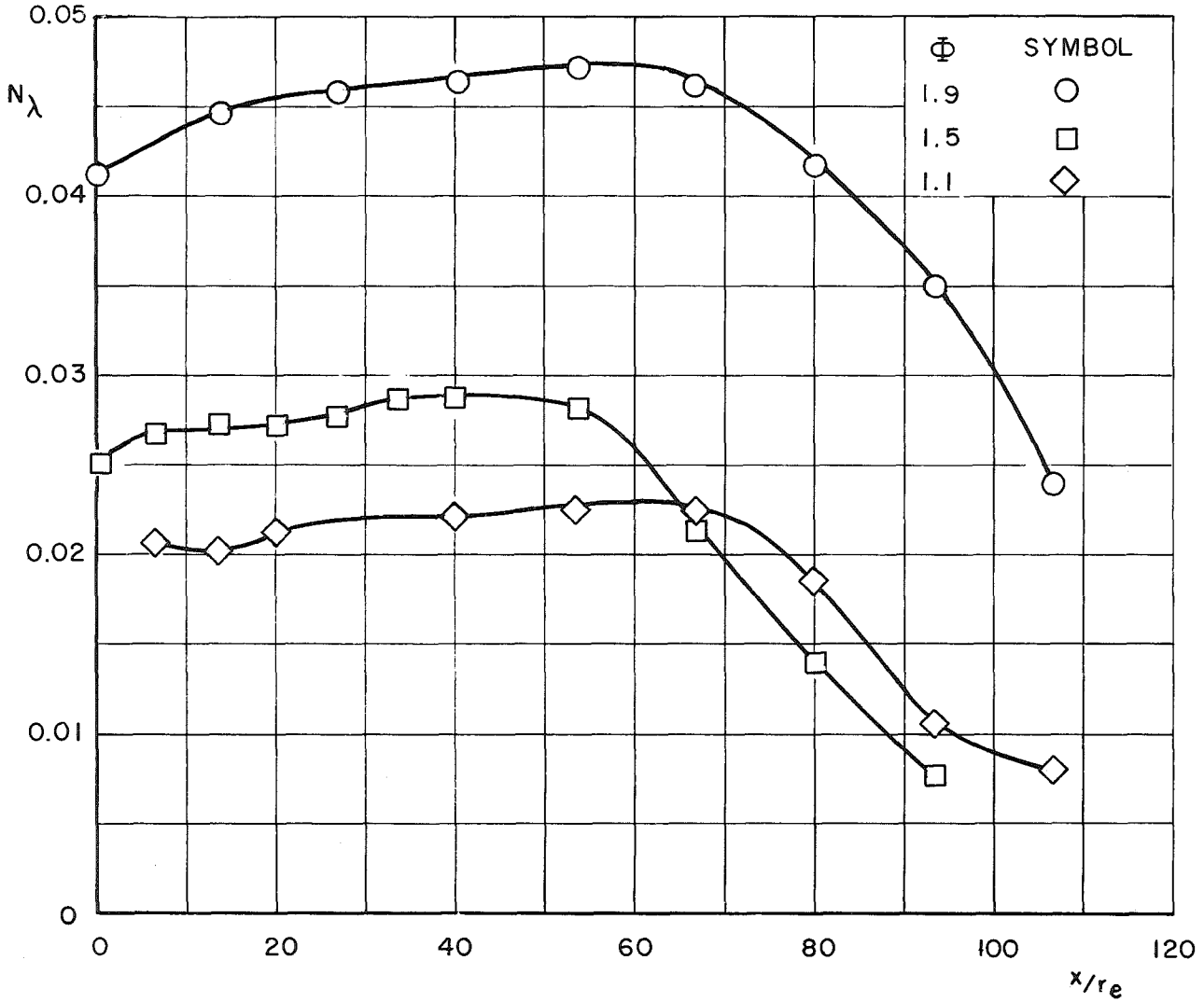

Fig. 17 Comparison of Rocket Engine Plume Centerline Spectral Radiance for Different Equivalence Ratios, 8 to 1 Area Ratio Rocket Engine, Oxygen/RP-1 Propellants, $M_\infty = 0$, Sea Level

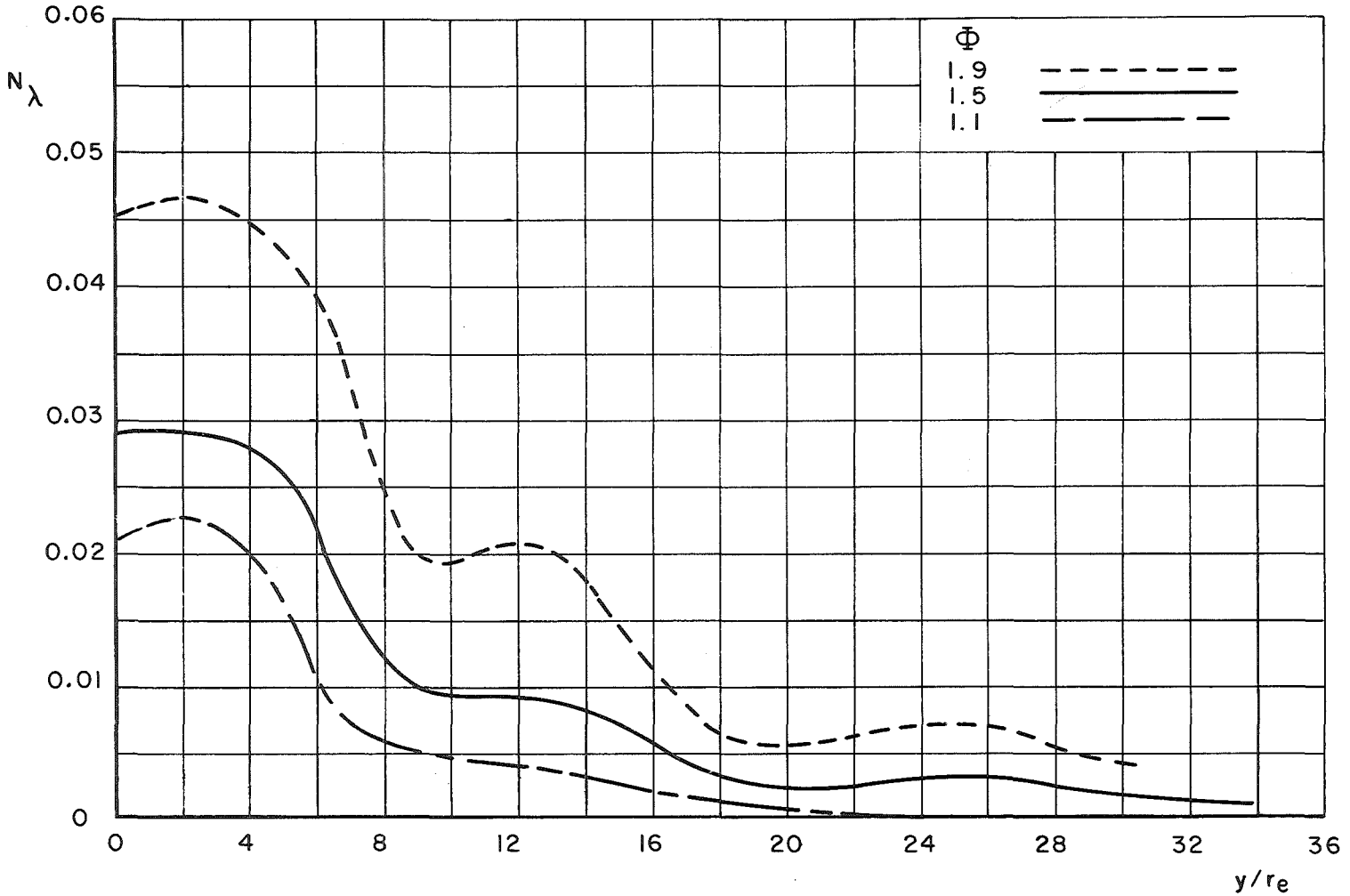

Fig. 18 Comparison of Spectral Radiance along a Rocket Plume Radius for Different Equivalence Ratios, 8 to 1 Area Ratio Rocket Engine, Oxygen RP-1 Propellants, $M_\infty = 0$, Sea Level, $x/r_e = 40$

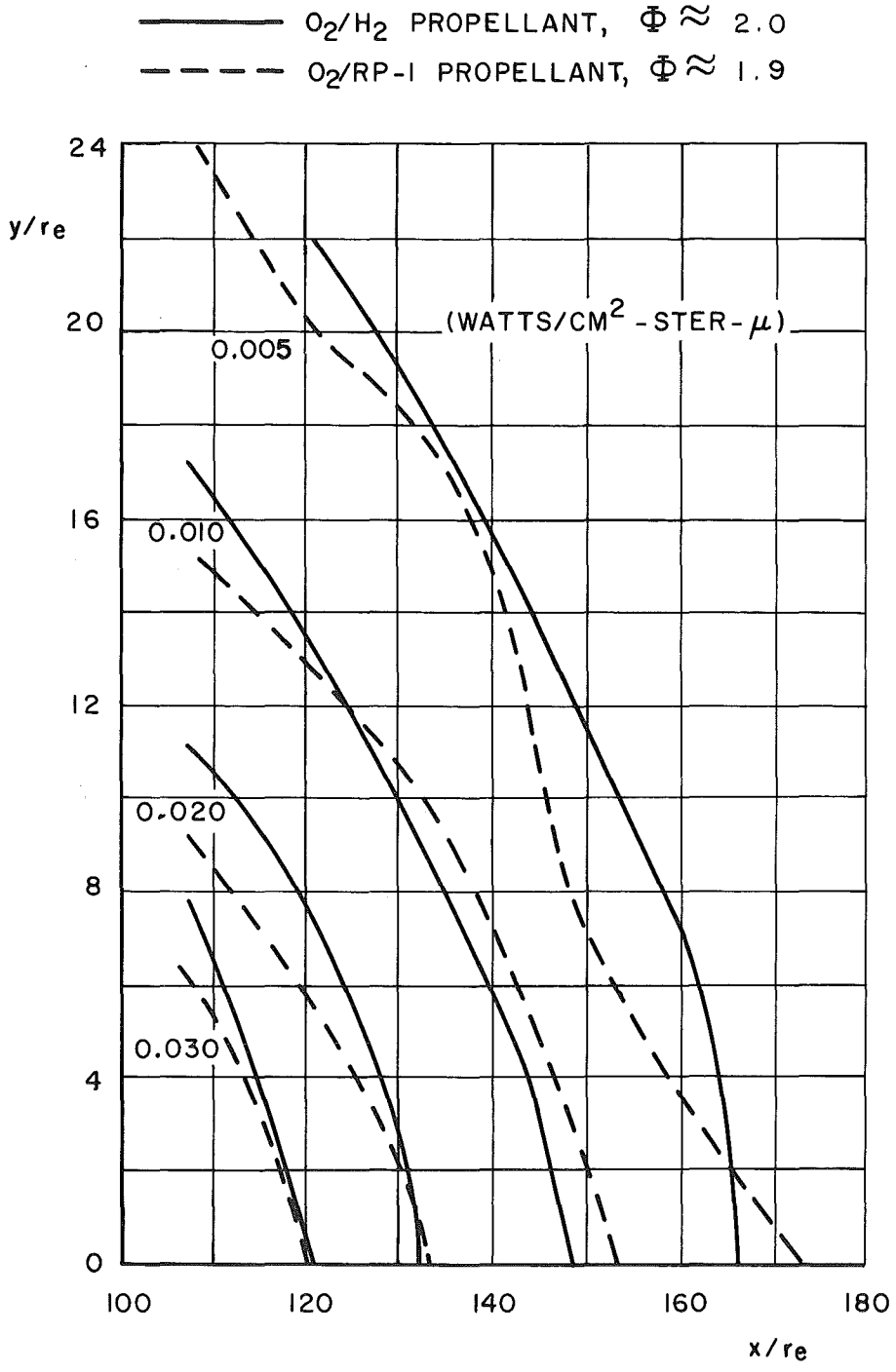

Fig. 19 Comparison of Isoradiance Curves for Oxygen/RP-1 and Oxygen/Hydrogen Propellants, 8 to 1 Area Ratio Rocket Engine, $M_\infty = 0$, Sea Level

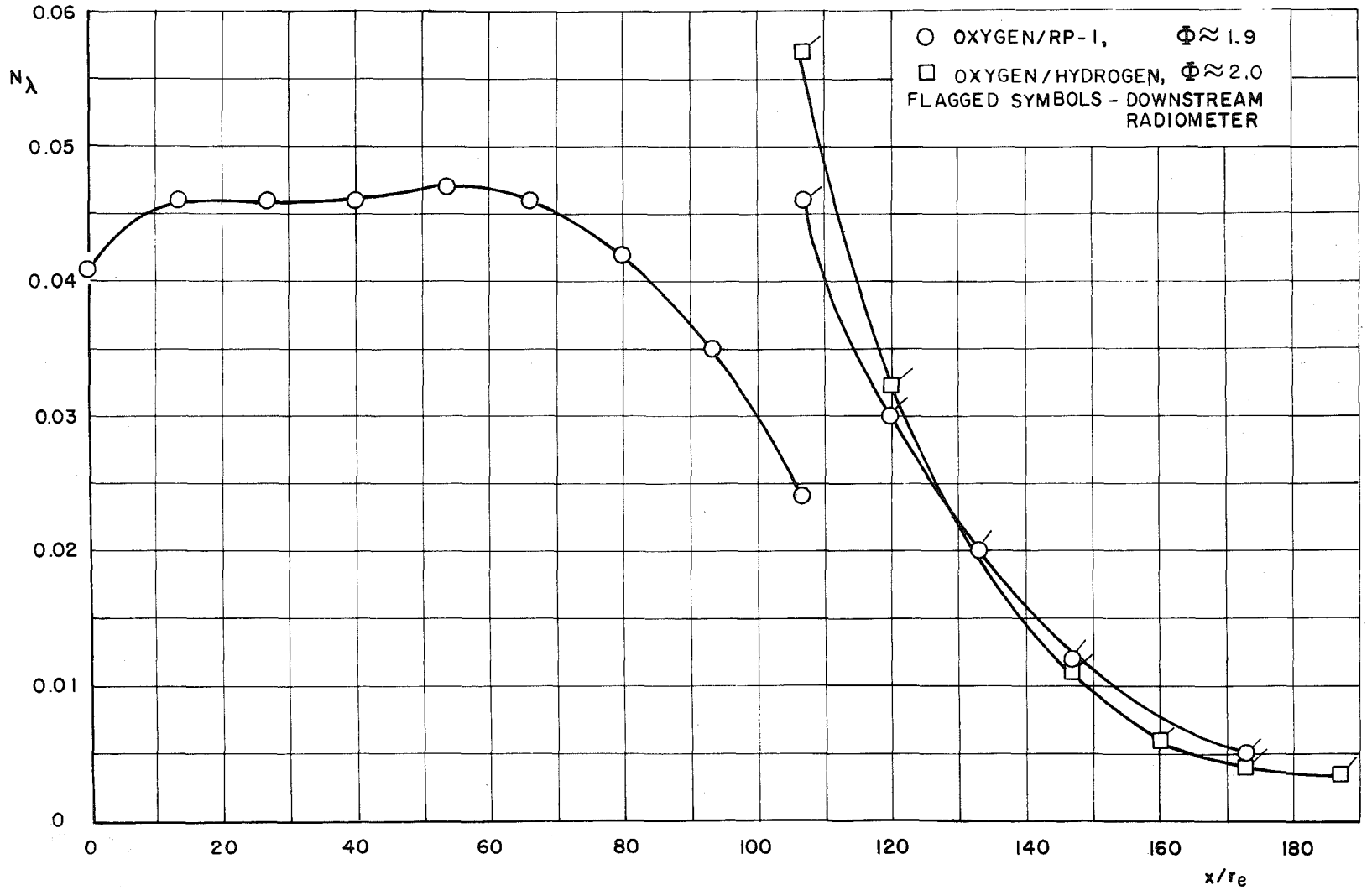

Fig. 20 Comparison of Rocket Plume Centerline Spectral Radiance for Oxygen /RP-1 and Oxygen/Hydrogen Propellants, 8 to 1 Area Ratio Rocket Engine, $M_\infty = 0$, Sea Level

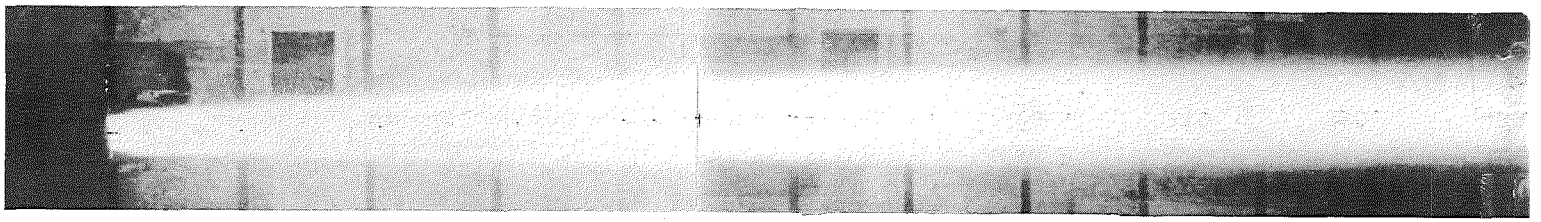

a. Visible Plume Photograph, $M_\infty = 1.75$, Z = 50,000 ft

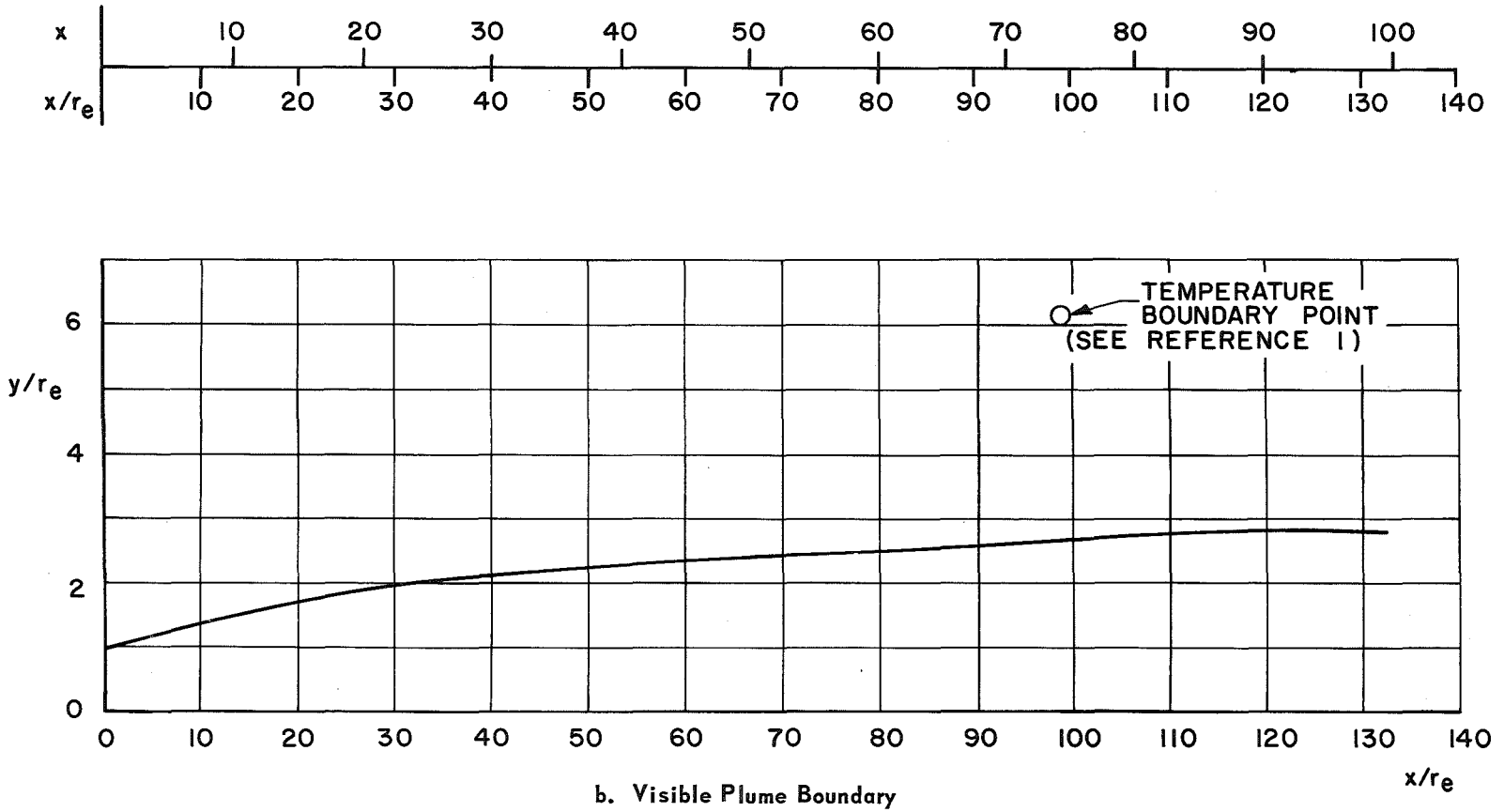

b. Visible Plume Boundary

Fig. 21 Photograph and Photographic Boundary, 25 to 1 Area Ratio Rocket Engine at Trajectory Conditions, Oxygen/RP-1 Propellants, $\Phi \approx 1.5$

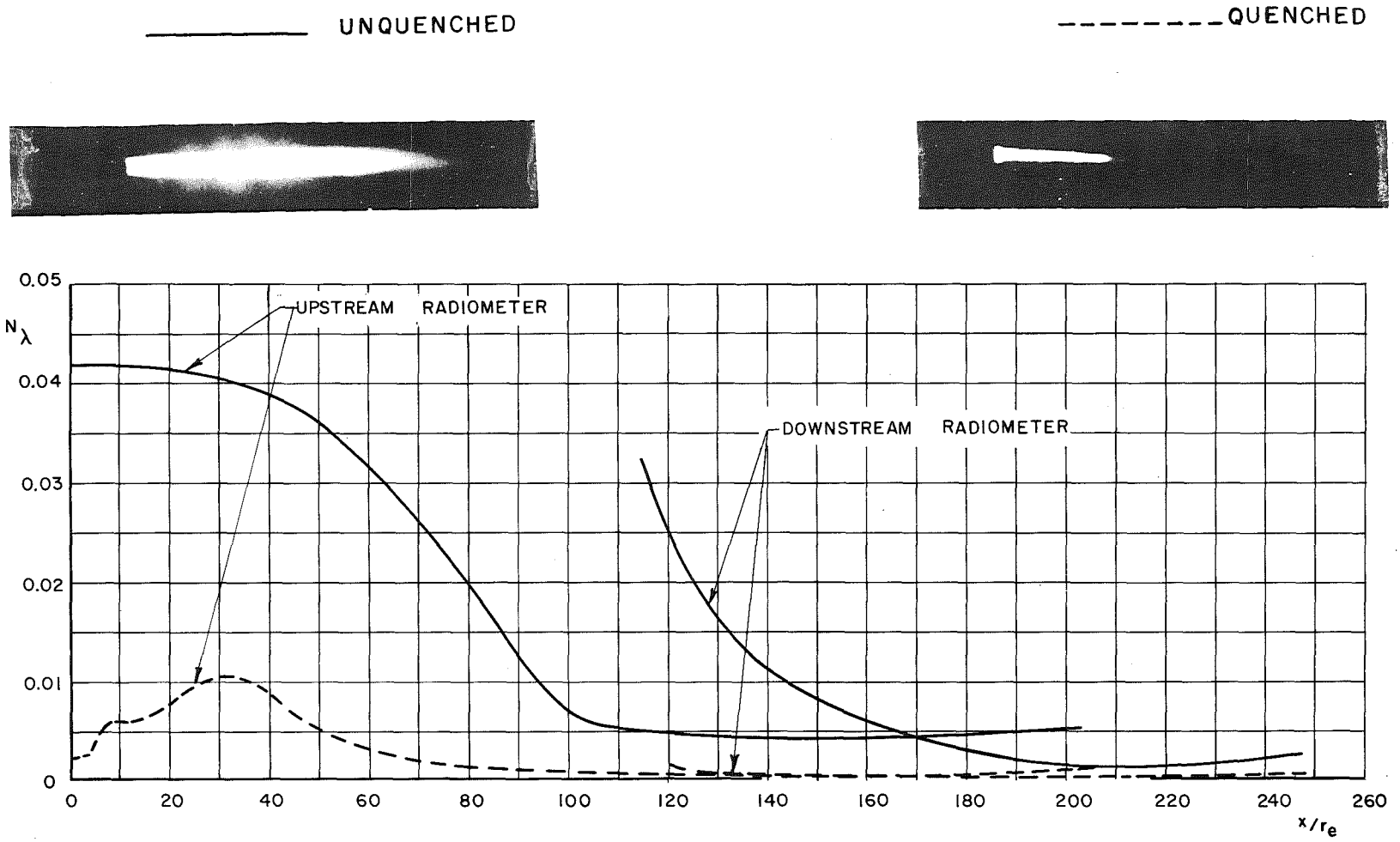

Fig. 22 Effect of Quenching upon Rocket Engine Plume Spectral Radiance, 8 to 1 Area Ratio Rocket Engine, Oxygen/RP-1 Propellants, $\Phi \approx 1.6$, $w_q/w_p = 0.45$, $M_\infty = 0$, Sea Level

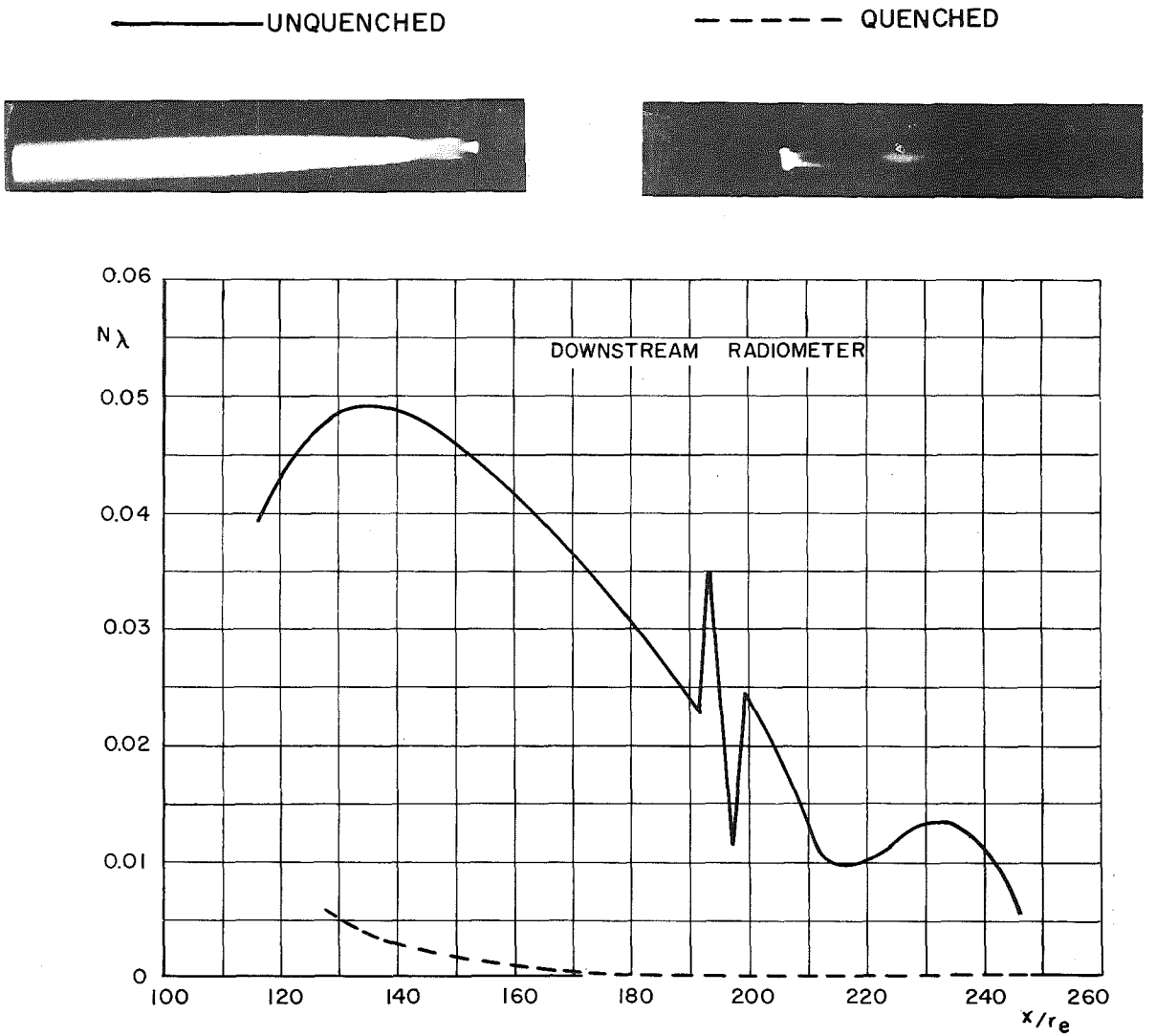

Fig. 23 Effect of Quenching upon Rocket Engine Plume Centerline Spectral Radiance, 8 to 1 Area Ratio Rocket Engine, Oxygen /RP-1 Propellants, $\Phi \approx 1.5$, $w_q/w_p = 0.28$, $M_\infty = 1.75$, Z = 50,000 ft

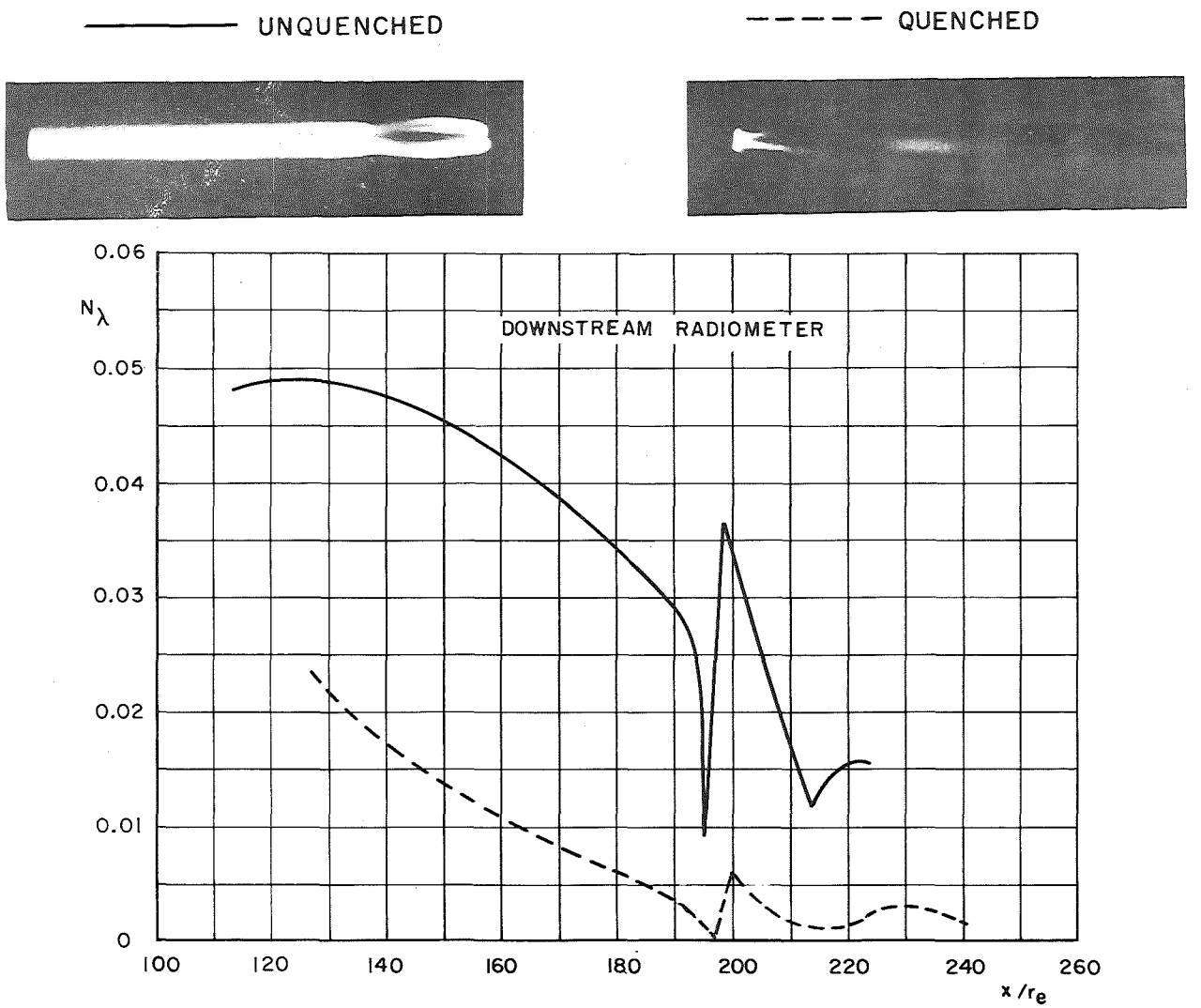

Fig. 24 Effect of Quenching upon Rocket Engine Plume Centerline Spectral Radiance, 8 to 1 Area Ratio Rocket Engine, Oxygen/RP-1 Propellants, $\Phi \approx 1.5$, $w_q/w_p = 0.20$, $M_\infty = 2.15$, $Z = 66{,}500$ ft